Korean Journal of Radiology

Emerging Techniques in Brain Tumor Imaging: What Radiologists Need to Know

Minjae Kim, MD, Ho Sung Kim, MD, PhD

All authors: Department of Radiology and Research Institute of Radiology, University of Ulsan College of Medicine, Asan Medical Center, Seoul 05505, Korea

Among the currently available brain tumor imaging, advanced MR imaging techniques, such as diffusion-weighted MR imaging and perfusion MR imaging, have been used for solving diagnostic challenges associated with conventional imaging and for monitoring the brain tumor treatment response. Further development of advanced MR imaging techniques and postprocessing methods may contribute to predicting the treatment response to a specific therapeutic regimen, particularly using multi-modality and multiparametric imaging. Over the next few years, new imaging techniques, such as amide proton transfer imaging, will be studied regarding their potential use in quantitative brain tumor imaging. In this review, the pathophysiologic considerations and clinical validations of these promising techniques are discussed in the context of brain tumor characterization and treatment response.

Keywords: *Brain; Neoplasm; Chemoradiotherapy; Perfusion; Diffusion; Magnetic resonance imaging*

INTRODUCTION

The use of advanced MR imaging techniques, such as diffusion-weighted MR imaging (DWI) and perfusion MR imaging, is rapidly expanding in the field of neuro-oncology for diagnosing brain tumors, guiding surgical procedures, as well as monitoring the tumor treatment response. Water diffusion is substantially decreased in the setting of increased tumor cellularity, and perfusion MR imaging

techniques assess tumor vascularity associated with neoangiogenesis. Recently, these have rapidly become the modalities of choice for detecting, characterizing or even staging viable tumor lesions, especially in malignant brain tumors, including glioblastomas, metastatic tumors, and lymphomas.

MR hardware, such as gradient coils used for advanced MR imaging, have been greatly improved recently and new MR techniques have emerged based on a variety of pathophysiologic backgrounds (1, 2). In DWI, intravoxel incoherent motion (IVIM) is entering the clinical field for evaluating tissue perfusion without the use of contrast agents and allowing separation of microcirculation from true water molecular diffusion (3). Diffusion kurtosis imaging (DKI) can analyze non-Gaussian diffusion through high diffusion weighting and is increasing the sensitivity to tissue features as well as providing information regarding the deviation from unrestricted diffusion associated with complex cytoarchitectonic environment (4). Perfusion MR imaging techniques have often been used in the evaluation of malignant brain tumors and consist primarily of three

methods: dynamic susceptibility contrast (DSC) perfusion MR imaging; dynamic contrast-enhanced (DCE) perfusion MR imaging; and arterial spin labeling (ASL). These three perfusion MR techniques definitely reflect different pathophysiologies and have different clinical impacts regarding the evaluation of pre- and post-treatment brain tumors. A relative cerebral blood volume (rCBV) derived from DSC perfusion MR imaging reliably estimates the tumor microvessel area (MVA) as a biomarker of the glioma outcome (5). DCE perfusion MR imaging is suitable for discriminating mature and immature tumor vessels in order to demonstrate the hypoxia-induced regulation of the tumor-vessel permeability (6). Cerebral blood flow (CBF) obtained using ASL may be useful for predicting tumor vascular normalization, especially following anti-angiogenic treatment. New imaging techniques, such as contrast-enhanced susceptibility-weighted imaging (CE-SWI) and amide proton transfer (APT) imaging, are now being used for investigating molecular and quantitative brain tumor imaging.

After a brief review of the specific pathophysiologic considerations of each advanced MR imaging technique, a review of the key areas of clinical validation will be discussed. Each review will specifically focus on currently outstanding issues regarding advanced brain tumor imaging, followed by some considerations regarding technical challenges.

Pathophysiologic Hot Spots and Consideration of Emerging Techniques of Brain Tumor Imaging

The Apparent Diffusion Coefficient Reflects Various Aspects of Tumors Not Just Tumor Cellularity

Diffusion-weighted MR imaging is sensitive to microscopic, subvoxel water motion for which an apparent diffusion coefficient (ADC) can be estimated, and reflecting the magnitude of water motion. However, the water molecules can be within extracellular, intracellular or intravascular space, all of which can differently contribute to the DWI signal as they have different speeds and anatomical and pathological barriers (Fig. 1). The ADC usually estimates water diffusion within the extracellular and extravascular space and has been shown to be inversely correlated with tumor cellularity (7, 8), and largely thought to be due to restriction of extracellular water motion due to the tightly packed tumor cells. Given that pre- and

post-treatment malignant brain tumors have a high tumor cellularity, they usually have low ADC values. In general, any effective pharmacologic or radioactive treatment that causes necrosis or cellular lysis will lead to less cellularity. As a decrease in the number of tumor cells in response to treatment obviously precedes tumor size change, DWI may, therefore, be an early biomarker for predicting treatment outcomes, monitoring the early treatment response, and detecting recurrent tumor. This DWI signal change associated with tumor cellularity can be enhanced with high b values which increase the effect on the signal of obstacles to the free diffusion present in tissue (Fig. 2) (9).

Although previous studies have shown an inverse correlation between tumor cell density and ADC (7, 8), high-grade gliomas are spatially and genetically heterogeneous. In particular, necrotic tumor components can show high DWI signals associated with tumor coagulation necrosis or ischemia (Fig. 3) (3). The restricted diffusion signal intensities can also be attributed to the combination of highly cellular tumor areas with inflammatory processes. Therefore, this heterogeneity can result in inadequate specificity for accurate tumor grading with the use of mean ADC values. In addition, DWI-derived ADC measures the average diffusion of water molecules within each voxel, and thus limiting the differentiation of active tumor from necrosis (10). Recent comparative studies showed that areas with restricted diffusion did not correlate with foci of high amino acid metabolism in human gliomas (11, 12). This discrepancy indicated that restricted diffusion may be affected not only by tumor cell density and metabolic activity but also other factors, such as ischemia or compression. In another previous study, as the ADC in metastatic brain tumors was associated with the histologic type of the primary cancer, the signal intensity on DWI could predict the histology of brain metastases (13).

Apparent Diffusion Coefficient Underestimates Tumor Cellularity in Hypervascular Tumors

Apparent diffusion coefficient values calculated using a monoexponential model may not be able to accurately reflect water molecular diffusion *in vivo* as it is influenced by the microcirculation of blood in capillaries (3). Therefore, the inverse relationship between the ADC value and tumor cellularity can be confounded by the factor of tumor vascularity. Both tumor cellularity and vascularity are higher in malignant brain tumors than in benign or low-grade tumors. High tumor cellularity can decrease the ADC
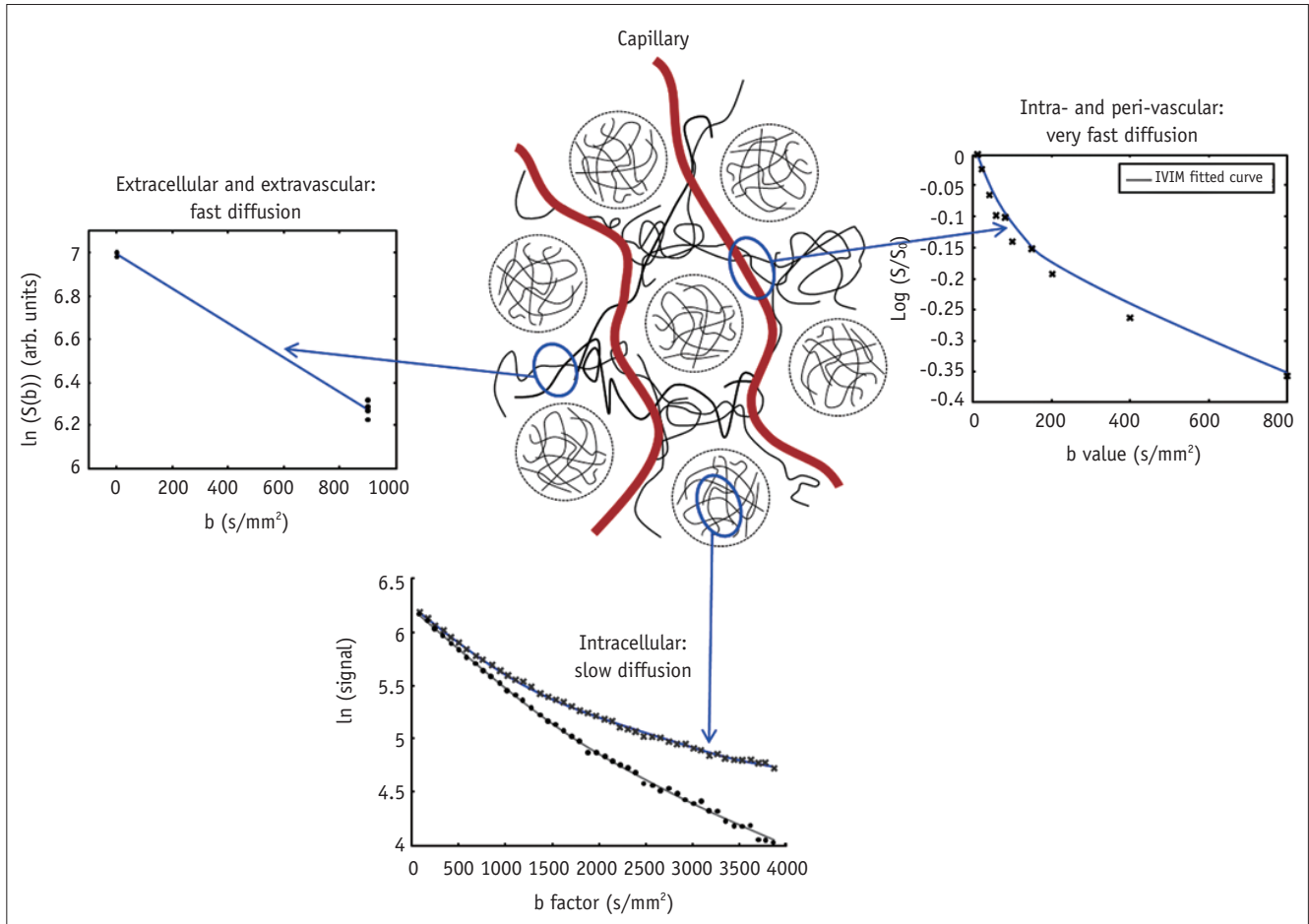
Fig. 1. Illustration of diffusion characteristics and their image processing. Fast diffusion within extracellular and extravascular space is calculated by monoexponential fitting of diffusion signals with b values of 0 and 1000 s/mm². Very rapid diffusion due to capillary perfusion can be characterized by biexponential fitting of diffusion signals as function of multiple b values, especially those less than 200 s/mm². Intracellular slow diffusion can be determined by biexponential fitting of diffusion signals with multiple high b values. IVIM = intravoxel incoherent motion

values, whereas high vascularity may increase the ADC, and which indicates that the DWI signal attenuation may be affected in opposite ways in hypervascular brain tumors. Therefore, ADC calculated from the monoexponential model may be limited for grading hypervascular brain tumors, and thus leading to contradictory results (14), whereas the IVIM-derived, true diffusion parameter may be more useful in characterizing tumor cellularity.

Intravoxel Incoherent Motion Separates Perfusion from Diffusion

The flow of blood water in randomly oriented capillaries mimics a pseudodiffusion which results in a signal attenuation in the presence of the diffusion-encoding gradient pulses. This pseudodiffusion effect is only seen at very low b values (< 200 sec/mm²) (3). Therefore, the biexponential model using multiple low b values, proposed by Iima and Le Bihan (3), might allow separation of

microcirculation from water molecular diffusion which may reflect the true diffusion coefficient.

The IVIM technique separately estimates parameter values for the perfusion effect, measuring DWI over multiple b values and using bi-exponential fitting. Under the assumed isotropic and random nature of the microvascular network system resulting in the incoherent motion of water in the blood, both capillary perfusion and true molecular diffusion can be separated using DWI with multiple b-values. In a pioneering study (15), IVIM was used to quantify perfusion in the human brain. IVIM MR imaging allows the simultaneous acquisition of diffusion and perfusion parameters which reflect tumor cellularity and vascularity, respectively, and it does not require any co-registration process between diffusion- and perfusion-based images. IVIM is also independent of the arterial input function for parameter quantification and does not require intravenous contract agent injection for the data acquisition.
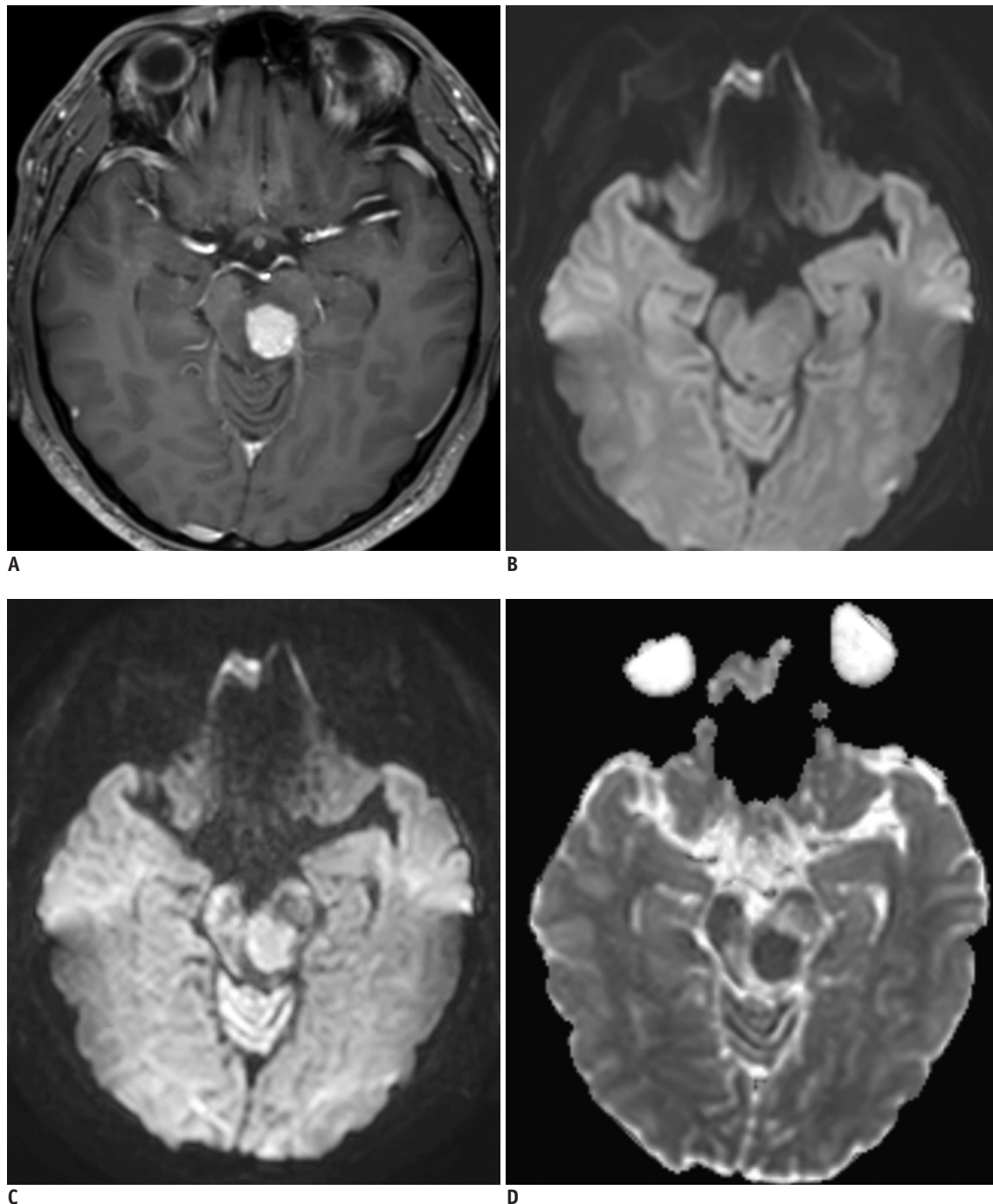
Fig. 2. DWI with low and high b values of presumed lymphoma in 38-year-old male.
A. Contrast-enhanced, axial, T1-weighted MR image shows contrast-enhancing mass in brain stem. **B.** DWI with b value of 1000 s/mm² shows equivocal high-signal intensity in same lesion. **C.** DWI with b value of 3000 s/mm² enhances DWI signal, high signal intensity in corresponding lesion. **D.** ADC is correspondingly low as DWI with higher b values increases effect on signal of obstacles to free diffusion present in tissue. ADC = apparent diffusion coefficient, DWI = diffusion-weighted MR imaging

On the contrary, separation of perfusion from diffusion requires high signal-to-noise ratios, and there are some technical challenges to overcome, such as artifacts from other bulk flow phenomena including vascular tubular flow and glandular secretion, which are difficult to separate from microcapillary perfusion (16). Another technical challenge may be that IVIM has a different sensitivity to vessel sizes, according to the range of b values.

Diffusion Kurtosis Imaging Estimates Cytoarchitectonic Complexities of Both Gray and White Matter

With free diffusion, the distribution of diffusion-driven
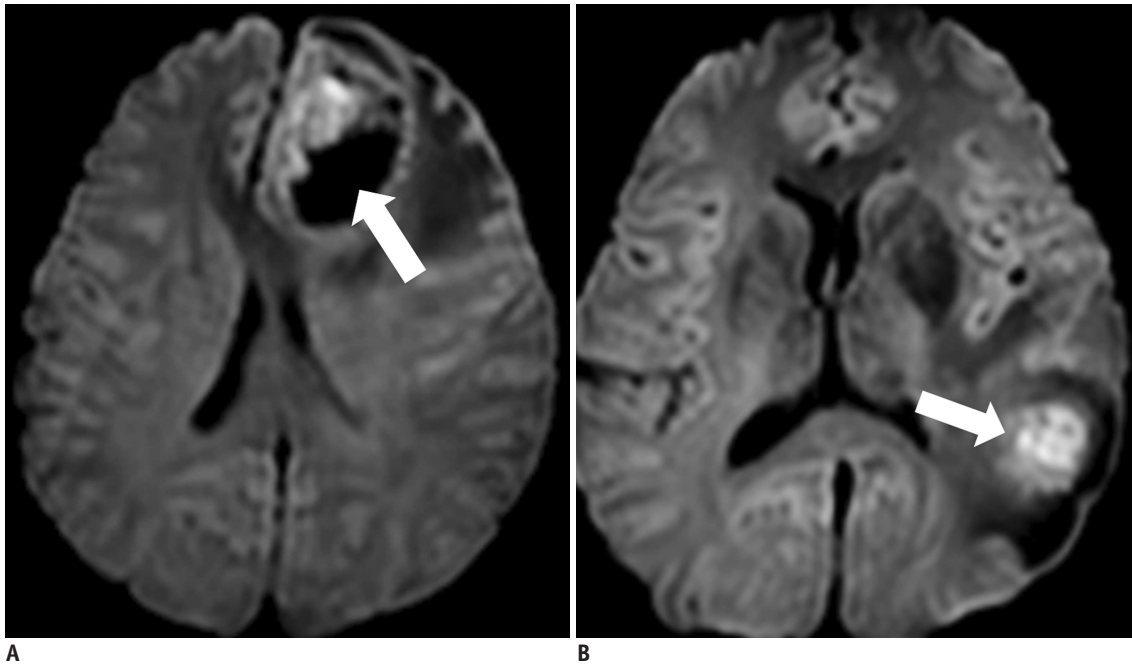
Fig. 3. Different DWI signals within tumor necrosis of two glioblastomas.
A. Necrotic tumor component of glioblastoma usually shows low DWI signal (arrow) due to migration and apoptosis of hypoxic tumor cells. **B.** Tumor necrosis could also show high DWI signal (arrow) due to tumor coagulation necrosis or ischemia associated with vascular occlusion by tumor cells. DWI = diffusion-weighted MR imaging

molecular displacements obeys the Gaussian law. However, in biologic tissue, the complex microstructures in biological tissue result in hindered and restricted diffusion of water molecules, and which leads to a non-Gaussian distribution (17). The non-gaussianity of water diffusion is thought to depend on cell membranes, organelles, and water compartments which represent the microstructure of the tissue (4). DKI has been used to measure non-Gaussian diffusion which has the potential to characterize both normal and pathologic tissue better than diffusion tensor imaging (DTI) (4). Compared to the DTI which describes the unrestricted but hindered anisotropic diffusion of water protons, DKI reflects unrestricted diffusion determined by the cytoarchitectonic complexity and can measure the degree of tissue organization (18). The mean kurtosis (MK) which is one of the principle DKI parameters, is thought to be an index of microstructural complexity. An advantage of MK over fractional anisotropy (FA) obtained on DTI is that as MK does not rely on spatially oriented tissue structures it can be used to characterize both gray and white matter (19, 20).

Increased values of the kurtosis parameters in high-grade gliomas may reflect a higher degree of tissue complexity resulting from tumor invasion, increased tumor cellularity, necrosis, hemorrhage, and endothelial

proliferation. Whereas low-grade gliomas usually have relatively homogeneous areas of tumor cells with sparse tumor-cell density, and thus resulting in lower kurtosis parameter values (21). Maier et al. (22) postulated that the difference between low-grade and high-grade gliomas may be attributable to the difference in the component size of the intra- and extracellular space rather than to a change in the diffusion characteristics of protons. This could possibly correspond with the presence of more densely packed membrane structures and cellular and myelin breakdown products in high-grade gliomas, whereas low-grade gliomas are composed of well-differentiated, neoplastic astrocytes on a loosely structured fibrocollagenous matrix with only moderately increased cellularity.

In terms of the technical consideration of DKI, the noise can be another cause of curvature of the signal attenuation than non-Gaussian diffusion at high b values. At high b values, because of the nature of the MR imaging signal, there is always some background noise signal remaining (23). Such noise effects can cause over- or underestimation of the model outputs, and should, therefore, be corrected.

Dynamic Susceptibility Contrast Perfusion MR Imaging Reflects Microvessel Density or Microvessel Area

Microvessel density (MVD) poorly characterizes the

morphometric complexity of large lumen microvessels of brain tumors. MVA, encompassing both the number and the caliber of the microvessels, can provide a better approach to the overall vascular surface area and, hence, may represent a more accurate measure of the degree of angiogenesis than MVD. The inverse correlation between MVD and size related parameters may be explained by an infiltrative tumor growth in cerebral grey matter, which is characterized by numerous delicate microvessels, as well as by the presence of glomeruloid vascular structures (24-26). Previous studies showed that MVA correlates more strongly with patient survival compared with MVD (25, 26). Glioblastomas are often characterized as having the predominance of either glomeruloid vessels representing high MVA or delicate, thin lumen, capillary-type vessels representing low MVA (26, 27). Glioblastomas lacking glomeruloid vessels have been associated with longer patient survival, and thus suggesting that tumor vessel morphology might be related to the
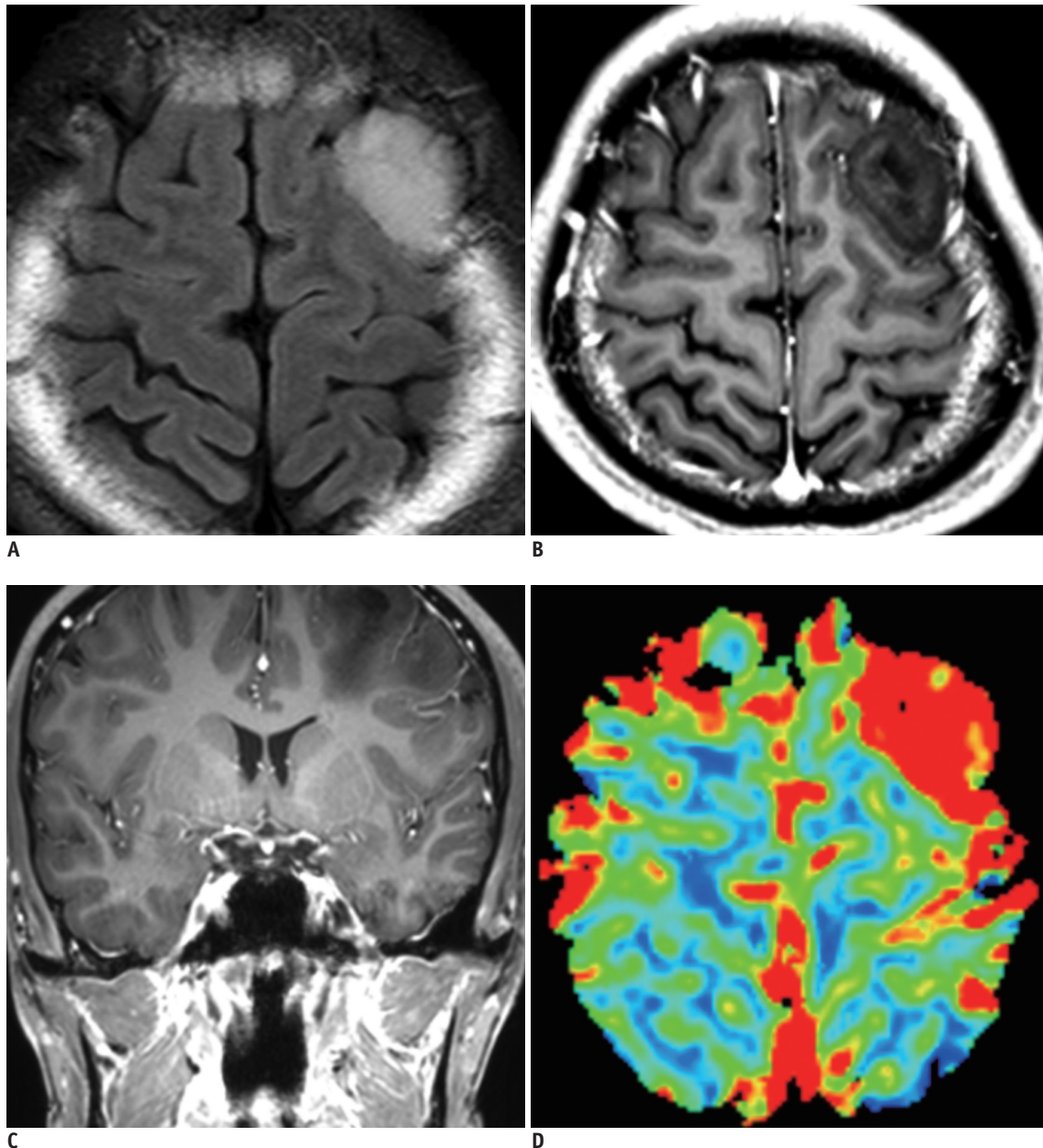
Fig. 4. Increased rCBV of anaplastic astrocytoma in 23-year-old male.
A. Intra-axial mass with high signal intensity seen on FLAIR, is noted in left frontal lobe. **B, C.** Mass dose not enhance on contrast-enhanced axial **(B)** and coronal **(C)**, T1-weighted MR images. **D.** rCBV map derived from DSC perfusion MR imaging shows markedly increased rCBV in corresponding lesion, and thus reflecting larger luminal area of tumor microvessels. DSC = dynamic susceptibility contrast, FLAIR = fluid attenuated inversion recovery, rCBV = relative cerebral blood volume

patient prognosis those with high-grade gliomas. Anaplastic gliomas can have an elevated MVA, thus reflecting large area, single-lumen microvessels and could exhibit MVA larger than that of glioblastoma (Fig. 4) (24-26).

Dynamic susceptibility contrast perfusion MR imaging is based on a first-pass bolus imaging technique generally used to estimate rCBV in brain tumor studies. For this purpose, this perfusion method uses T2*-weighted MR acquisition to enhance the magnetic susceptibility effects of gadolinium-based contrast agents. A previous investigation showed that rCBV could reflect tumor vascular morphometry (28). Although MVA undoubtedly represents a more clinically relevant parameter (25), to date nearly all rCBVs have been correlated using MVD data from animal models (29, 30). Therefore, whether rCBV more strongly reflects MVD versus MVA directly impacts the utility of rCBV as a clinical predictor of the glioma outcome (24, 26, 27). A previous human study reported that rCBV reliably estimates tumor MVA as a biomarker of the glioma outcome, but poorly estimates MVD in the presence of vessel size heterogeneity inherent to glioblastomas (5).

On the other hand, the tumor vessels of posttreatment brain tumors usually show contrast agent leakage through the extensively disrupted blood-brain barrier, and resulting in additional T1 or T2* relaxation effects in the extravascular space. The T2* contrast-agent leakage effects that depend on the density and spatial distribution of tumor cells within the extracellular extravascular space can also lead to an additional susceptibility calibration factor (31,

32). Therefore, within the complex microenvironment of post-treatment brain tumors, and where vascular integrity and architecture are known to be highly heterogeneous, estimation of the rCBV might be less reliable than estimation of the T1 kinetic parameters (Fig. 5).

Dynamic Contrast-Enhanced Perfusion MR Imaging Identify Immature Hyperpermeable Vessels

A further way of studying tumor vessel characteristics is to assess the permeability of gadolinium-based MR contrast agents. DCE perfusion MR imaging applies a pharmacokinetic model to determine the exchange of contrast agents between the intravascular compartment and the extravascular, extracellular compartment (1, 33, 34). The transfer coefficient (K_{trans}) derived from the pharmacokinetic model is associated with the tumor-vessel surface area and its permeability. As the extravasation of contrast agents in brain tumors is mostly attributed to immature hyperpermeable vessels, it is suitable for discriminating mature and immature tumor vessels and for showing the hypoxia-induced regulation of tumor-vessel permeability, both of which might be potential biomarkers of tumor progression in brain tumors (6).

Compared with DSC perfusion MR imaging, DCE perfusion MR imaging usually requires more complex data acquisition and analysis. First, determination of T1 values in brain tissue before contrast injection is required for calculation of tissue contrast concentration curve with time (35). Second, an accurate measurement of arterial input

A   **B**   **C**
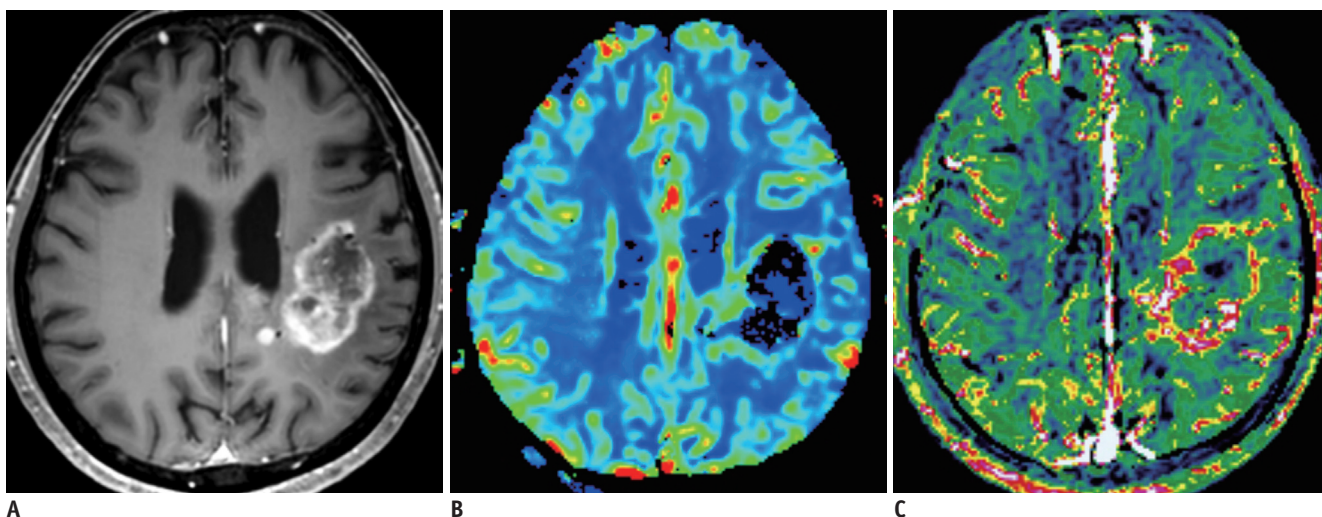
Fig. 5. Images obtained in 63-year-old female clinicoradiologically considered as having recurrent glioblastoma.
A. Contrast-enhanced, T1-weighted image acquired 17 months after concomitant chemoradiotherapy, shows necrotic, enhancing mass in left parietal lobe. **B.** DSC perfusion MR image shows equivocal increase of rCBV in corresponding lesion. **C.** Corresponding, contrast-enhanced, solid portion shows definite increase of permeability on DCE perfusion MR imaging, and thus suggesting tumor recurrence. DCE = dynamic contrast-enhanced, DSC = dynamic susceptibility contrast, rCBV = relative cerebral blood volume

function is needed but is difficult to obtain because the relationship between MR signal intensity and absolute contrast concentration is not always linear and might be compromised by inflow (36). Nevertheless, three-dimensional acquisition of DCE MR imaging allows a higher signal-to-noise ratio and spatial resolution and can, therefore, provide accurate characterization of tumor vascular permeability patterns (Fig. 6). In addition, DCE MR imaging is more sensitive to small vessel function than other imaging modalities. These advantages may be useful in terms of monitoring drug delivery, compared with other imaging modalities. Theoretically, the pharmacokinetic model derived from DCE perfusion MR imaging can allow the evaluation of tumor drug delivery, thereby also allowing assessment of the therapeutic response to chemotherapeutic drugs. Consequently, DCE perfusion MR imaging can be an adequate noninvasive method for assessing the tumor vascular pattern and acceptable surrogate markers of hypoxia-induced tumor angiogenesis (37).

Arterial Spin Labeling Predicts Tumor Vascular Normalization and Drug Delivery Efficacy

The tumor vascular characteristics might be associated with the therapeutic response as the specific patterns of the tumor vessels could enhance or reduce chemotherapeutic drug delivery to the tumor cells (38, 39). For example, several previous studies regarding tumor response to

antiangiogenic treatment have demonstrated that tumor blood perfusion measurements may be helpful in predicting tumor treatment response by showing that higher perfusion could be associated with favorable outcome (40, 41). One explanation for this association might be that as high CBF reflects less permeable tumor vessels and an increase of the tumor perfusion fraction, and thus resulting in efficient chemotherapeutic drug delivery to the target tumor cells (Fig. 7), after which the clinical outcome would be better.

Arterial spin labeling is a noninvasive method of quantifying CBF that magnetically labels blood water as an endogenous tracer without contrast agent injection (42). ASL has been proven to be reliable and reproducible in the assessment of CBF in various pathologic states and has also been reported to correlate with tumor blood-vessel attenuation and the glioma grade (43, 44). Therefore, ASL which is a completely noninvasive method of determining tumor blood flow, would be highly desirable, particularly if there is a correlation between the CBF and the clinical outcome measures, including patient survival.

Contrast-Enhanced Susceptibility-Weighted Imaging Characterizes Tumor Necrosis and Vessels

Susceptibility-weighted imaging (SWI) is an emerging MR imaging technique which uses a 3-dimensional, T2*-weighted gradient echo sequence that combines magnitude and filtered-phase information (45). SWI has the potential
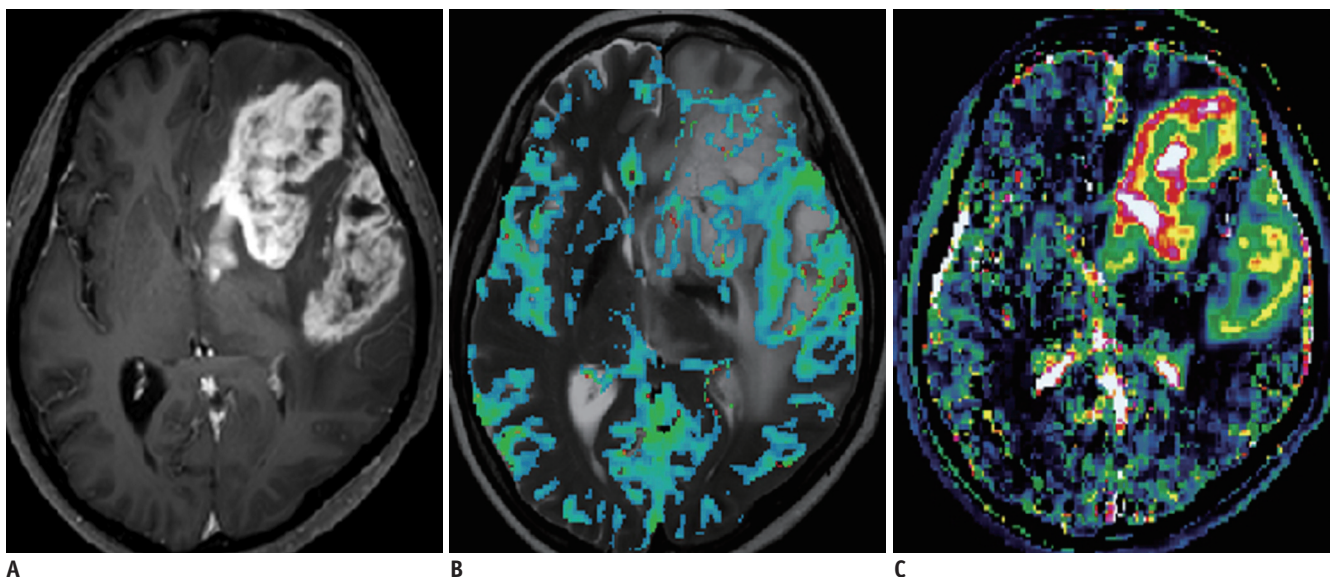
Fig. 6. Comparison of DSC and DCE perfusion MR images in 67-year-old female with glioblastoma.
A. Contrast-enhanced, axial, T1-weighted MR image shows necrotic, contrast-enhancing mass in left frontal and temporal lobes. **B.** DSC perfusion MR imaging shows heterogeneously increased rCBV in corresponding lesion. **C.** DCE perfusion MR imaging shows higher signal-to-noise ratio and spatial resolution of permeability distribution within same lesion, compared with that seen on DSC perfusion MR imaging. DCE = dynamic contrast-enhanced, DSC = dynamic susceptibility contrast, rCBV = relative cerebral blood volume
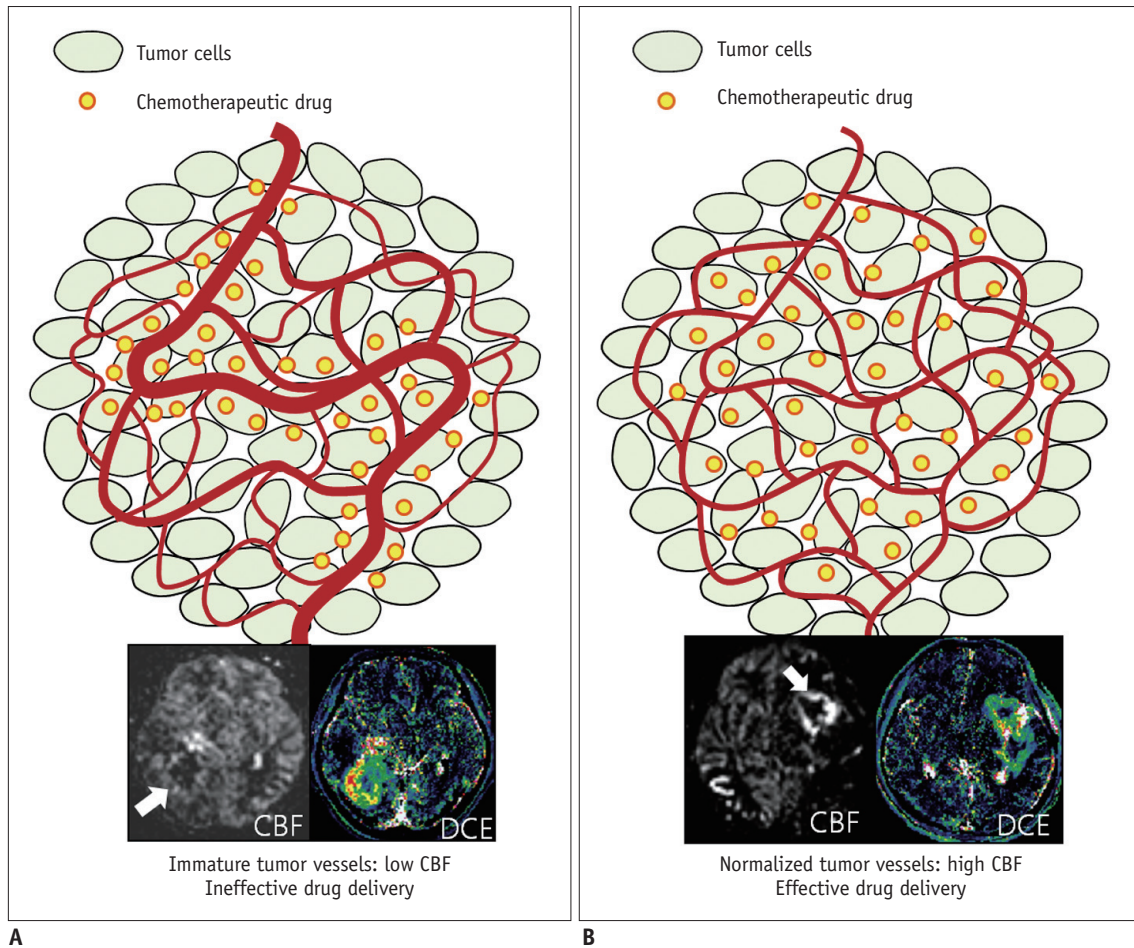
Fig. 7. Illustration of association between tumor vessel pattern and cerebral blood volume.
A. Immature, hyperpermeable, and tortuous tumor vessel pattern causes ineffective and heterogeneous tumor blood flow (arrow) which thus impedes delivery of chemotherapeutic drug to tumor. **B.** Increased homogeneity of tumor-vessel density and more well ordered arrangement of vessels increase tumor blood flow (arrow) and reduce its heterogeneity, and which improve drug delivery and efficacy. CBF = cerebral blood flow, DCE = dynamic contrast-enhanced

to visualize cerebral veins without contrast medium injection as well as visualizing microhemorrhage (46). SWI can visualize T2 effects, such as edema and contrast enhancement, associated with T1 shortening effects as well as T2* effects (47). With SWI, the internal architecture of a tumor can be better defined compared with to that seen on conventional, contrast-enhanced, T1-weighted images. To characterize tumor necrosis, the internal architecture of tumors varies significantly on SWI and contrast-enhanced T1 imaging (Fig. 8). The internal architecture seen on contrast-enhanced T1 is determined by the presence of necrosis, cysts, and tumor boundaries, whereas the internal architecture seen on SWI is primarily determined by blood products and/or tumor vessels (46).

The use of gadolinium-based contrast agents has been proposed in order to improve the characterization of susceptibility signals inside brain mass lesions (48). Some

susceptibility signals can be depicted on both SWI and CE-SWI, although some susceptibility signals are only visible on CE-SWI. Hemorrhage can also be distinguished from veins if SWI is used both before and following the administration of a contrast agent (46). Blood vessels will change their signal intensity before and after administration of a contrast agent, whereas regions of tumoral hemorrhage appear unchanged (Fig. 9). The tumoral hemorrhage which is easily seen on CE-SWI can cause misregistration of DSC perfusion MR images into structural MR images for quantitative analyses. Therefore, CE-SWI might be advantageous as high-resolution, structural MR imaging for contrast-enhancing tumor segmentation, compared with contrast-enhanced, T1-weighted imaging.

In another previous study using CE-SWI (49), stereotactic biopsies of two different kinds of susceptibility signals were performed on one patient. On the histological results,
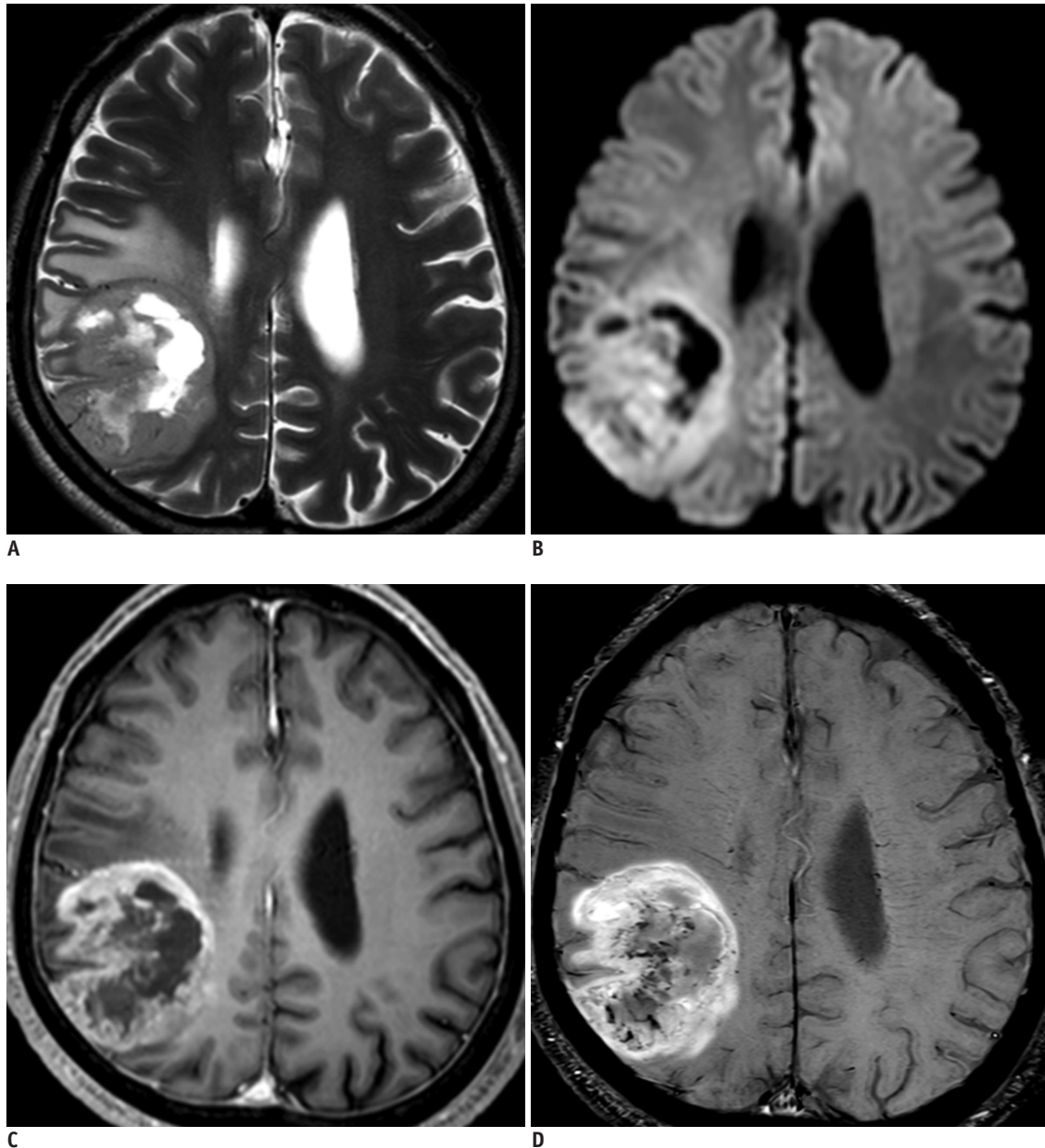
Fig. 8. Images obtained in 76-year-old male with glioblastoma.
A. T2-weighted MR image shows intra-axial mass with surrounding edema in right parietal lobe. **B.** DWI shows high signal intensity in corresponding lesion, and thus suggesting high tumor cellularity. **C.** Contrast-enhanced, axial, T1-weighted MR image shows necrotic, contrast-enhancing mass in same lesion. **D.** Contrast-enhanced SWI shows additional information regarding microhemorrhage and tumor microvessels around tumor necrosis seen on contrast-enhanced, T1-weighted image. DWI = diffusion-weighted MR imaging, SWI = susceptibility-weighted imaging

the area of intratumoral susceptibility signals on pre-contrast SWI contained highly pathological vessels, micro-hemorrhage, and extensive necrosis. On the other hand, the susceptibility signals which were visible only on CE-SWI were present in the tumor invasion zone, defined as a loss of tumor-cell density at the margins of the specimen due to migration of tumor cells along fiber tracts into the surrounding brain tissue (50).

Amide Proton Transfer Imaging Is a Potential Biomarker for Tumor Proliferation

Amide proton transfer imaging is a variant of chemical exchange saturation transfer (CEST) imaging in which the magnetization of the "proton of interest" is detected indirectly through the chemical exchange with bulk-water protons (Fig. 10) (51, 52). It is a noninvasive MR imaging technique sensitive to endogenous mobile proteins
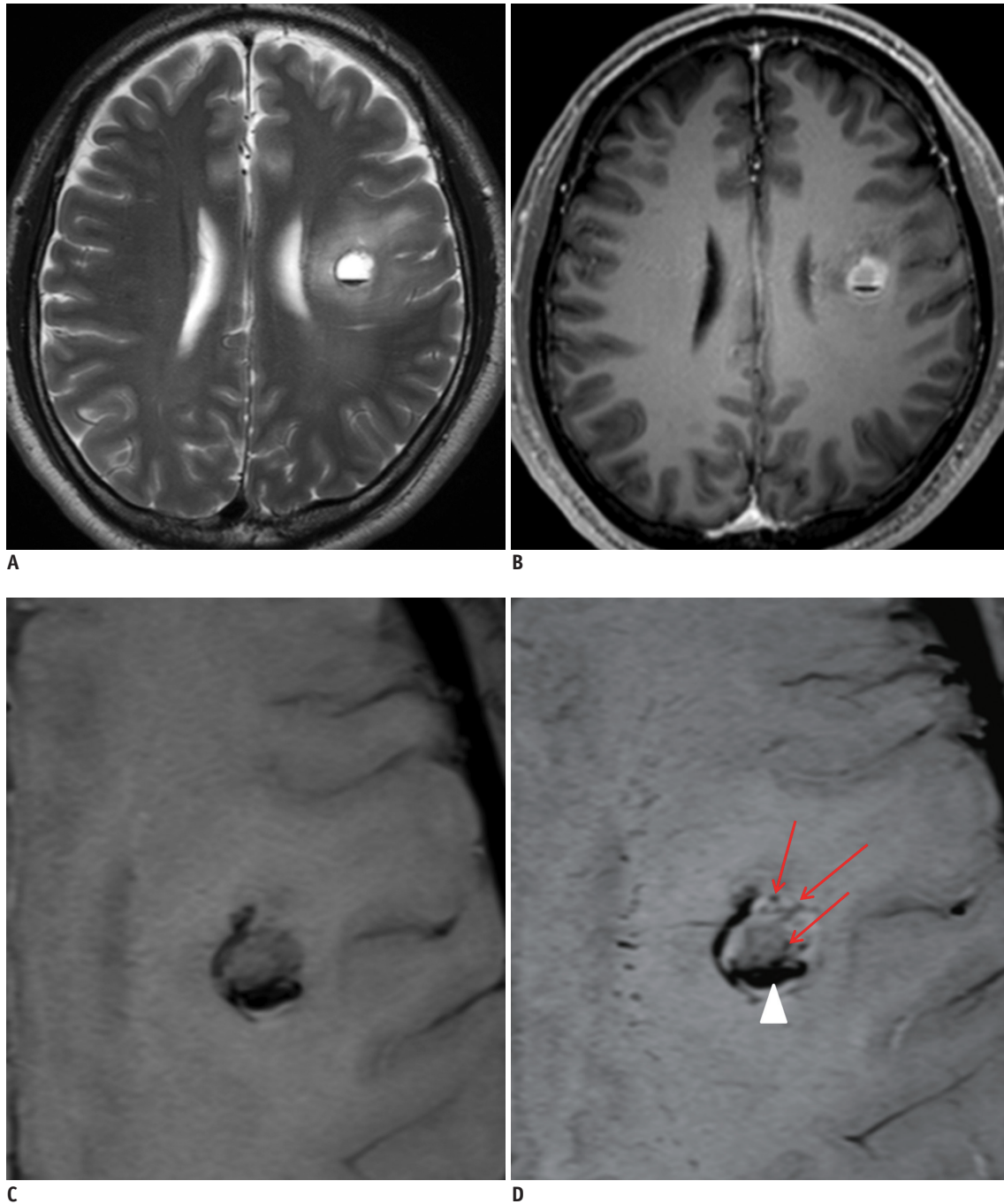
Fig. 9. Images obtained in 47-year-old male with anaplastic oligodendroglioma.
A, B. T2-weighted MR image **(A)** and contrast enhanced, T1-weighted image **(B)** show intra-axial lesion with internal hemorrhage in left frontal lobe. **C.** Pre-contrast SWI demonstrates rim of low signal intensity in corresponding lesion. **D.** Contrast-enhanced SWI shows additional linear or dot-like structures of low signal intensity (arrows), suggesting tumor microvessels as well as unchanged lesion of low signal intensity (arrowhead), and suggesting microhemorrhage. SWI = susceptibility-weighted imaging

and peptides and has been introduced as a potentially useful technique that reflects tumor-cell proliferation and provides information regarding the pH of tissue (53, 54). Quantitative APT parameters have been proposed as prognostic indicators of brain gliomas by reflecting the cellular proliferation levels that correlated with Ki-67 (55)

and as a sensitive biomarker of treatment responses (56) in experimental and clinical studies. Therefore, compared with DWI and perfusion MR imaging, APT imaging has a potential to provide completely different biologic information on molecular changes and tumor proliferation index. As molecular events precede the morphologic changes,
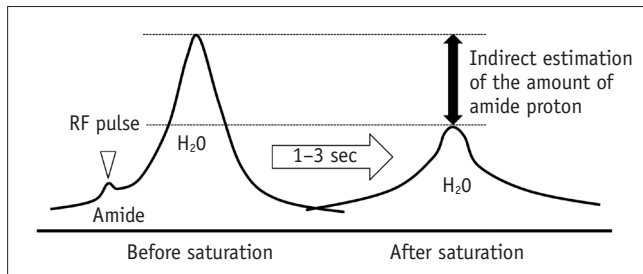
Fig. 10. Illustration of amide proton transfer mechanism.
Amide protons are saturated at their specific resonance frequency with selective radiofrequency pulse. Saturated proton is then transferred to surrounding free water and consequently water signal decrease is calculated for indirect estimation of amount of amide proton.

observing changes in endogenous molecules can provide valuable information in treatment response. This is why APT imaging could be a complementary imaging biomarker in the glioma studies despite of its inherent technical limitations. Compared with other advanced imaging parameters, the APT parameter shows different distribution due to the different pathophysiologic background (Fig. 11). This would provide more accurate targets for stereotactic biopsy and local therapies in patients with glioma (57).

There have been recent technical advances in APT imaging that allow whole-brain, three-dimensional acquisition within a reasonable imaging time (53). Three-dimensional APT imaging seems to be a promising approach that can allow evaluation of an entire lesion. This is difficult with MR spectroscopy which is the currently practical method for endogenous metabolite imaging as it is limited by its low spatial resolution, long imaging time, and high operator dependency.

Current Clinical Hotspots of Emerging Imaging Techniques in Patients with Brain Tumors

Apparent Diffusion Coefficient: Monitoring Response to Antiangiogenic Treatment

Early changes in the ADC have been shown to be predictive of the long-term patient response to radiation and chemotherapies for brain tumors. Specifically, a previous study showed that an ADC increase following cytotoxic chemotherapies could be associated with a favorable treatment response and might offer added value in identifying tumors that are responsive to cytotoxic chemotherapies (58, 59). The ADC has the potential to serve as a surrogate marker for emerging treatment response efficacy (Fig. 12). Results from a previous study clearly indicate that pretreatment ADC histogram analysis

is a predictive imaging biomarker for antiangiogenic therapy, but not for chemotherapy, within the context of a recurrent glioblastoma. Therefore, the use of ADC histogram analysis for recurrent glioblastomas can guide the use of antiangiogenic therapy in second-line therapy (60).

Intravoxel Incoherent Motion: Assessing Real Tumor Cellularity

A key feature of IVIM MR imaging is that it does not require contrast agents and it may serve as an interesting alternative to perfusion MR imaging in some patients with contraindications to contrast agents or patients with renal failure at risk for nephrogenic systemic fibrosis (61) or for gadolinium deposits in brain basal ganglia (62).

In our previous study (14) using a mono-exponential fitting which does not consider the contribution of the perfusion effect on diffusion signal decay, the ADC was significantly lower in the lymphoma group than in the other tumor patient groups. However, using a bi-exponential fitting which considers the contribution of the perfusion effect, the mean IVIM-derived, true diffusion parameter did not differ significantly between the lymphoma and the other tumor groups. This result indicates that the ADC difference between the lymphoma and the other tumor groups could be associated with the contribution of the perfusion effect on diffusion signal decay. Based on these results, we suggest that a monoexponentially fitted ADC which contains the perfusion effect may limit the reliability of the inverse correlation between the ADC and tumor cellularity. According to other previous studies (63, 64), the IVIM-derived perfusion parameters were correlated with rCBV derived from DSC perfusion MR imaging, and their histogram analyses may help in differentiating recurrent tumor from the treatment effect in glioblastoma.

Diffusion Kurtosis Imaging: Accurate Glioma Grading

As an extension of DTI, DKI can provide an additional measurement of MK to characterize the complexity of the tumor architectures and has the potential to allow measurement of the non-Gaussian diffusion in brain tumors. According to a previous study (65), both the water molecular diffusion heterogeneity index (α) and the MK had significantly greater diagnostic performance than did the conventional diffusion parameters, including ADC, the mean diffusivity, and FA, in differentiating low-grade gliomas from high-grade gliomas, and which was in agreement with other recent studies (17, 66). As such, DKI-derived
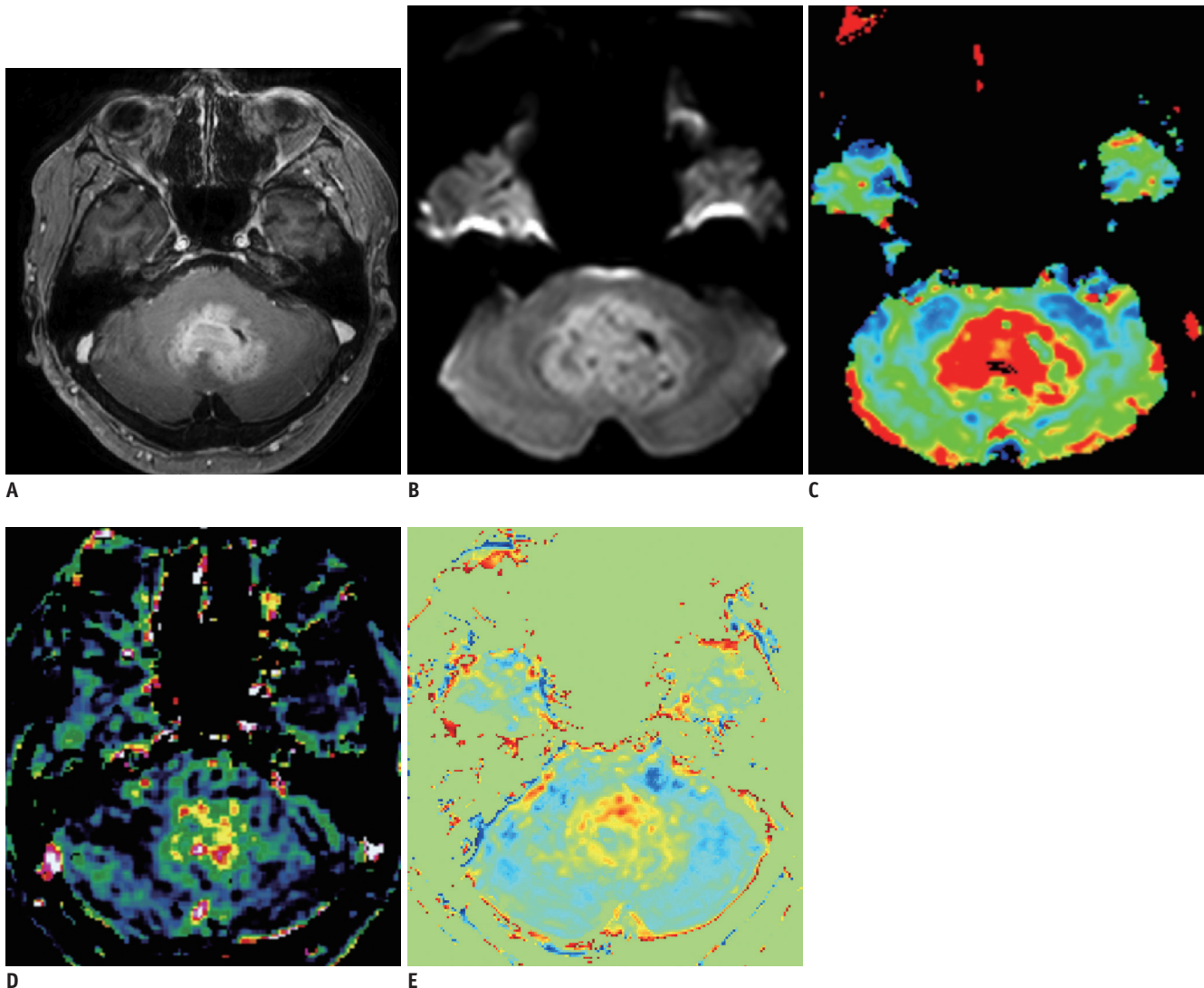
Fig. 11. Images obtained in 55-year-old male with glioblastoma.
A. Contrast-enhanced, axial, T1-weighted MR image shows contrast-enhancing lesion around fourth ventricle. **B-E.** All of advanced MR images including DWI **(B)**, DSC perfusion MR image **(C)**, DCE perfusion MR image **(D)**, and amide proton transfer image **(E)** show increased parametric values, although different distribution within corresponding contrast-enhancing lesion. DCE = dynamic contrast-enhanced, DSC = dynamic susceptibility contrast, DWI = diffusion-weighted MR imaging

diffusion parameters may serve as an optimal diffusion parameter for grading gliomas in clinical practice because other diffusion parameters such as FA derived from DTI, might not be accurate enough to reflect the actual non-Gaussian diffusion distribution in biological tissue (66).

Dynamic Susceptibility Contrast Perfusion MR Imaging: Exclusion of Pseudoprogression in Clinical Trials

The detection of transiently enlarging, contrast-enhanced lesions after chemoradiotherapy in patients with glioblastomas may influence the decision of whether to continue current therapy or change to a second-line therapy (67, 68). In addition, the eligibility in salvage treatment

trials has been limited due to the incorrect interpretation of the pseudoprogression. Therefore, for clinical trials, exclusion of pseudoprogression is essential in order to minimize the false-positive effect of a new drug (69). When differentiating between early tumor progression and pseudoprogression, the accuracy of the histopathologic diagnosis based on second-look surgery can be subject to sampling errors (70). Therefore, therapeutic strategies usually depend on both the interpretation of MR imaging findings as well as clinical manifestations.

Dynamic susceptibility contrast perfusion MR imaging has been investigated for differentiating between early tumor progression and pseudoprogression (69, 71, 72). According

to a previously published report, the percentage change of rCBV between the pre- and post-radiation-temozolomide therapies could be predictive of one-year patient survival (73). In another previous study, a parametric response map obtained from rCBV was able to distinguish therapy-associated pseudoprogression from true tumor progression in patients with high-grade glioma and a reduction in rCBV

three weeks after therapy was found to be an early predictor of true tumor progression (74). In our previous study, the early tumor progression patient group had negative changes of skewness and kurtosis of rCBV histograms during the short-term follow-up periods after concomitant chemoradiotherapy, whereas the pseudoprogression group did not (Fig. 13) (71). Despite the feasibility of applying
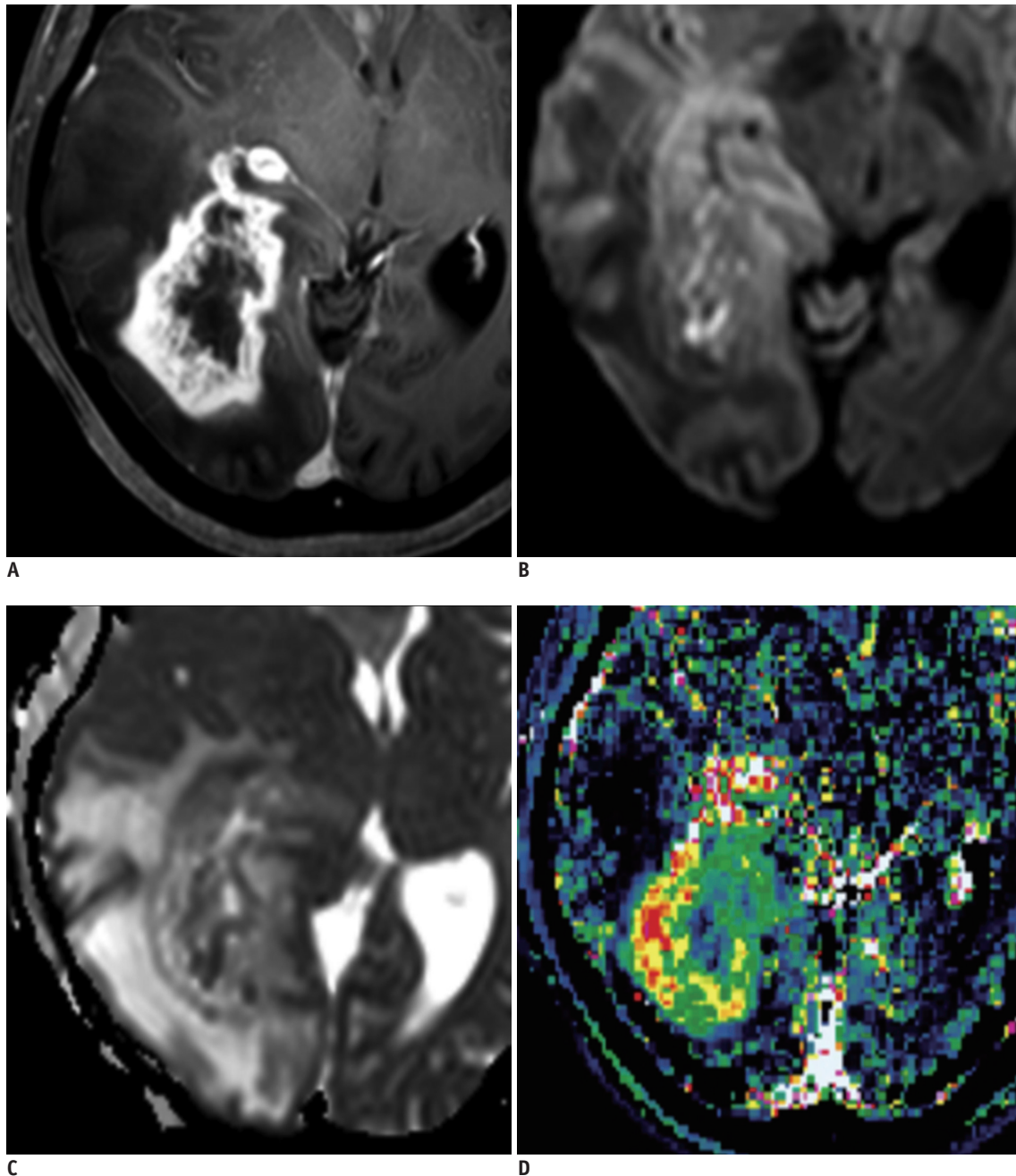
Fig. 12. Images obtained in 57-year-old female with recurrent glioblastoma.
A. Contrast-enhanced, T1-weighted image acquired five months after concomitant chemoradiotherapy shows necrotic, enhancing mass in right temporo-occipital lobe. **B, C.** DWI **(B)** and ADC **(C)** show linear area of diffusion restriction surrounding tumor necrosis, possibly indicating viable, compact tumor cells. **D.** DCE perfusion MR image shows increase of permeability in corresponding, contrast-enhancing lesion around area of diffusion restriction, and reflecting immature tumor vessel. ADC = apparent diffusion coefficient, DCE = dynamic contrast-enhanced, DWI = diffusion-weighted MR imaging
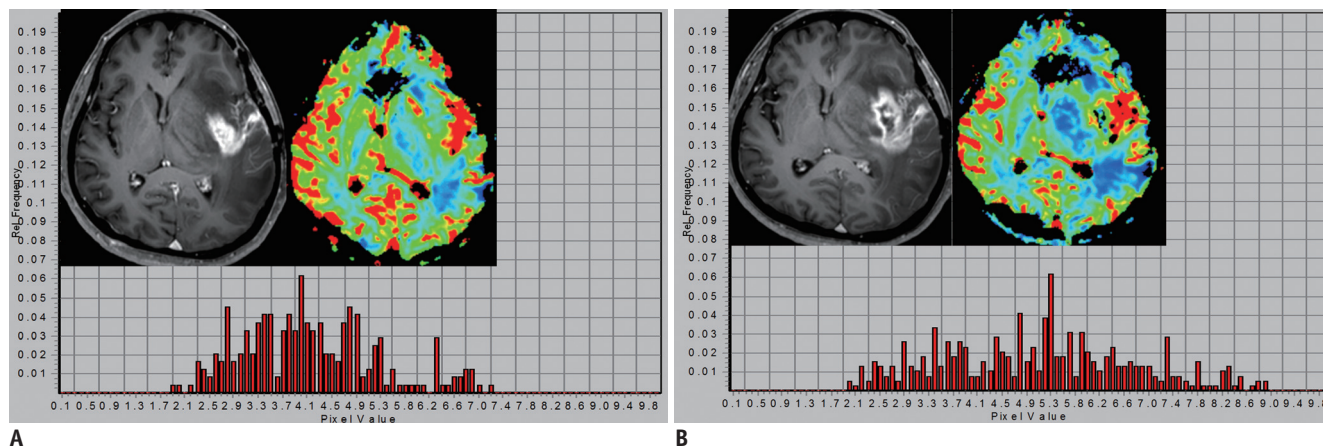
Fig. 13. Images obtained in 55-year-old female with recurrent glioblastoma.
A. At seven weeks after concomitant chemoradiotherapy, histogram from normalized rCBV for entire, corresponding, contrast-enhancing lesion reveals heterogeneous distribution of normalized rCBV values. **B.** At 15 weeks after concomitant chemoradiotherapy, histogram showed more heterogeneous distribution of normalized rCBV values compared with those seen in previous study, and thus suggesting tumor progression. rCBV = relative cerebral blood volume

the rCBV ratio in clinical practice, relying on this measure remains a matter of concern as many tumor progressions are intermingled with the post-treatment effect, especially in post-treatment glioblastomas. Nevertheless, DSC perfusion MR imaging can provide methods for differentiating pseudoprogression from true tumor progression as vascular proliferation is characteristic of tumor progression.

Dynamic Contrast-Enhanced Perfusion MR Imaging: An Adjunct to Dynamic Susceptibility Contrast Perfusion MR Imaging in Treatment Response Assessment

Dynamic contrast-enhanced perfusion MR imaging has demonstrated considerable utility for assessing microcirculation physiology in new vessel regeneration (75). Its application in oncology has been particularly recommended in a workshop report regarding noninvasive monitoring of both tumor progression and treatment response (76). Our previous results (77) regarding the initial area under the DCE time-signal intensity curve (IAUC) for differentiating recurrent glioblastoma from radiation necrosis, are consistent with previous results that showed the importance of initial vascular phase assessment to successfully differentiate tumor progression from treatment-related change (78). These consistent results might be explained by the fact that the IAUC depends mostly on the blood flow as well as on the total vascular surface area exposed to the contrast agent. Therefore, recurrent glioblastoma has a prominent IAUC that is based on hypervascularity and neoangiogenesis.

In our previous study, adding DSC or DCE perfusion MR imaging to the combination of conventional MR imaging

and DWI significantly improved the diagnostic performance for distinguishing recurrent glioblastoma from radiation necrosis (77). This result suggests that the MR imaging protocol that includes conventional MR imaging, DWI, and any perfusion MR imaging is most efficient in the accurate determination of recurrent glioblastoma, as compared with that includes the combination of conventional MR imaging and DWI. We found that the best overall diagnostic accuracy and the highest interreader agreement in the prediction of recurrent glioblastoma were achieved with a combination of conventional MR imaging, DWI, and DCE MR imaging.

Arterial Spin Labeling: The Efficacy of Tumor Drug Delivery

During tumor angiogenesis, the resulting tumor vessels are highly abnormal and immature, both structurally and functionally. Antiangiogenic treatment would prune some abnormal vessels and remodel the remaining vessels by blocking vascular endothelial growth factor signaling and thus resulting in a normalized vasculature. In turn, this would increase the CBF and reduce tumor hypoxia and interstitial fluid pressure, thereby resulting in enhanced efficacy of the tumor drug delivery. Therefore, the patients whose tumor perfusion increased during chemotherapy might survive longer than the other patients (40).

In our preliminary clinical study, there were clinically relevant differences in the treatment effect of cytotoxic chemotherapeutic agents between the positive-CBF and negative-CBF groups in patients with post-treatment glioblastoma (Fig. 14). There was a moderate advantage in the median time-to-progression (TTP) in the positive-

CBF cohort, compared with the negative-CBF cohort. On multivariate analyses, positive CBF was independent of the MGMT promoter methylation status for predicting longer TTP and a favorable clinical outcome. Our study verifies that the increased CBF is a reflection of hyperperfusion and evenly distributed tumor vessels, both of which mimic "normalized tumor vessels" seen in post-antiangiogenic treatment, and can indicate increased drug delivery to the tumor cells (39).

Contrast-Enhanced, Susceptibility-Weighted Imaging: Additional Value to Tumor Grading

The development of SWI allows improved contrast and detection of both the venous vasculature and hemorrhage within tumors, and which cannot be seen using conventional imaging methods (79). There is evidence that the use of SWI in the non-invasive grading of primary brain tumors by assessment of intratumoral susceptibility signal (ITSS) has been demonstrated (80, 81). High-grade tumors such as glioblastomas often have a hemorrhagic component and increased microvascularity which can be detected with the help of SWI.

In our previous study (80), the degree of ITSS showed a significant correlation with the value of the maximum rCBV in the same tumor segments. However, the direct correspondence between the areas of ITSS and the maximum rCBV was variable. Moreover, SWI demonstrated the highest
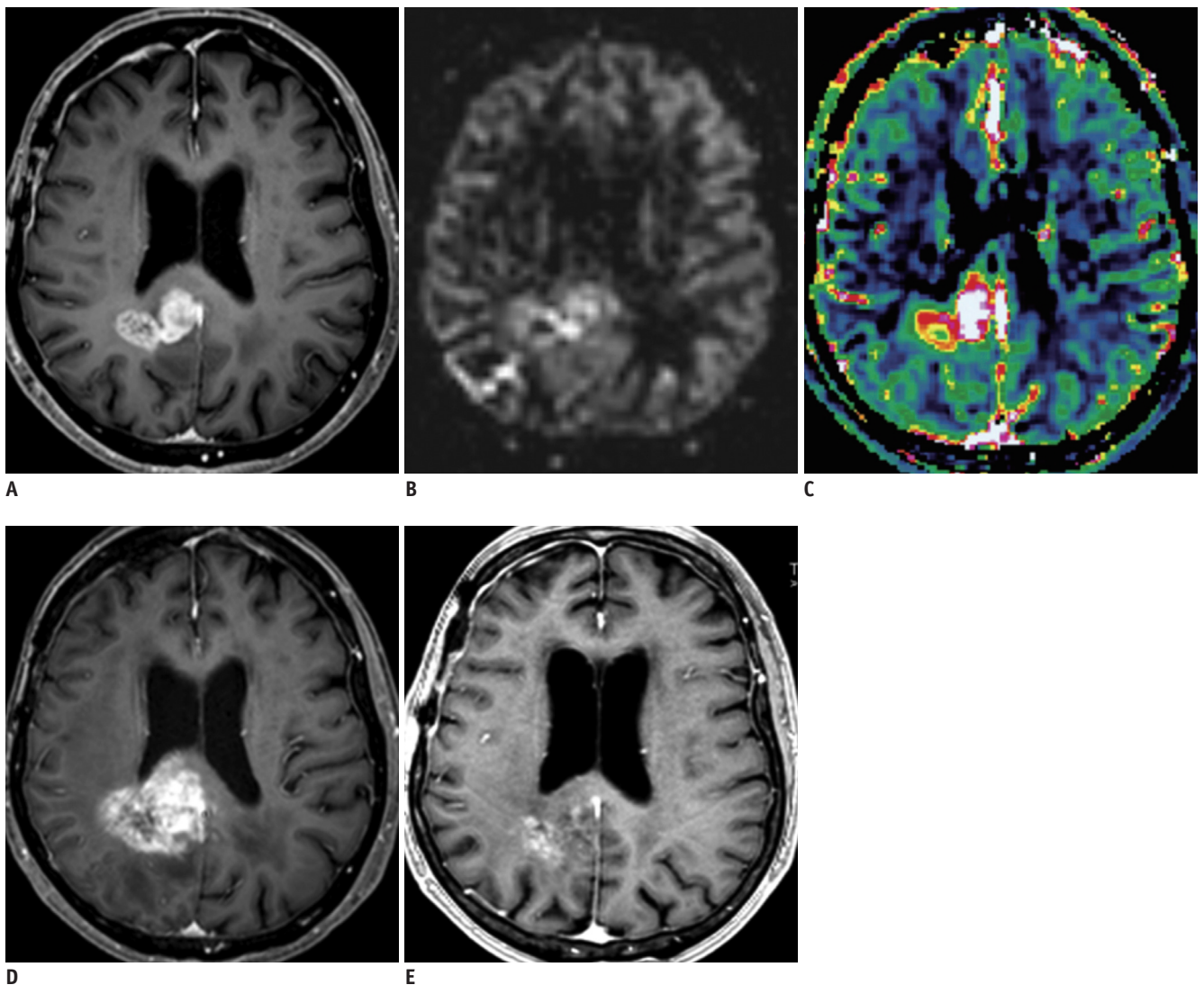
Fig. 14. Images obtained in 75-year-old female with pseudoprogression.
A. Contrast-enhanced, T1-weighted image acquired five weeks after concomitant chemoradiotherapy shows enhancing mass in right parieto-occipital lobe. **B, C.** ASL **(B)** and DCE perfusion MR imaging **(C)** show increased CBF and permeability in corresponding contrast-enhanced lesion, respectively, and thus indicating effective drug delivery. **D.** After two cycles of adjuvant temozolomide, extent of enhancing lesion increased. **E.** After four cycles of adjuvant temozolomide, enlarged, enhancing lesion was stabilized, and thus suggesting pseudoprogression. ASL = arterial spin labeling, CBF = cerebral blood flow, DCE = dynamic contrast-enhanced
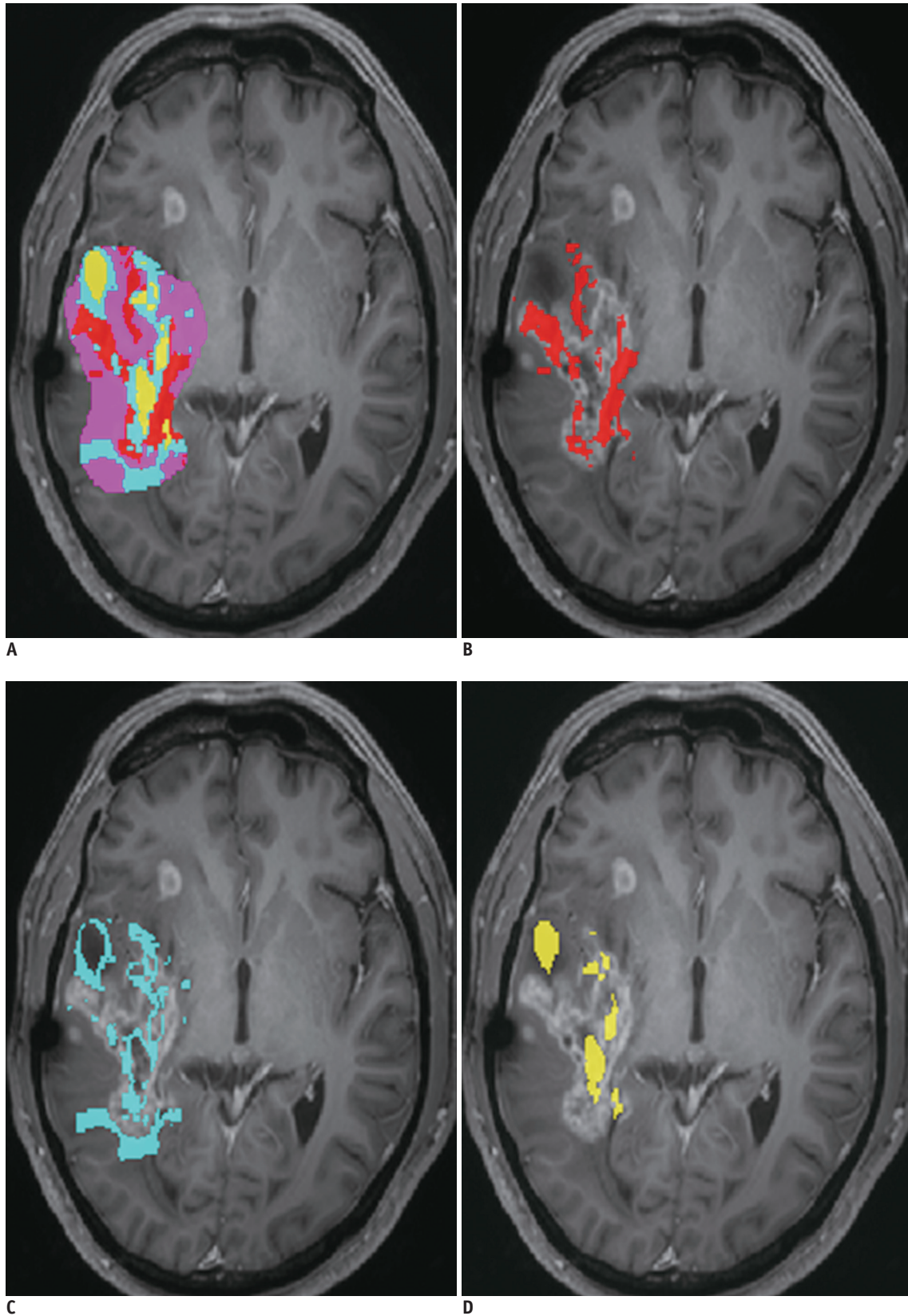
Fig. 15. Tumor clustering in 59-year-old female with recurrent glioblastoma.
A. Contrast-enhancing mass is segmented and clustered with combination of ADC, rCBV, and permeability parameters on voxel-by-voxel basis. **B.** Volume fraction of presumed tumor cluster is highest (45%), compared with other clusters **(C, D)**, and thus suggesting tumor recurrence. ADC = apparent diffusion coefficient, rCBV = relative cerebral blood volume

degree of ITSS in glioblastoma, thus suggesting that ITSS can be a potentially helpful sign for the correct diagnosis of high-grade gliomas. Our previous study also showed that the diagnostic performance of SWI for grading gliomas was comparable with that of DSC perfusion MR imaging (80). It has also been acknowledged that CE-SWI might offer additional information in the evaluation of brain tumors by depicting contrast enhancement as well as a greater multitude of susceptibility signals than non-contrast SWI (82).

Amide Proton Transfer Imaging: Potential Biomarker of Early Treatment Response

The authors of several, published studies (14-16) have shown that APT imaging allows the detection and characterization of malignant brain tumors. In addition, APT asymmetry values have been proposed as prognostic indicators of brain glioma as they reflect the cellular proliferation levels that correlate with Ki-67 (17), and function as sensitive biomarkers of treatment response (18) in experimental and clinical studies.

In our clinical experience, APT imaging showed a potential for being an imaging biomarker of the tumor-cell proliferative index to reflect different tumor biology. Histogram analysis of APT imaging provided an added value to DSC perfusion MR imaging for identifying contrast-enhancing, low-grade tumors mimicking high-grade tumors (83). In terms of the tumor proliferative index, APT imaging showed a moderate correlation with MR spectroscopy and was a superior imaging methodology, particularly for assessing post-treatment gliomas, compared with MR spectroscopy (57). Our other previous study showed that adding APT imaging to conventional and perfusion MR imaging improved the diagnostic performance for differentiating tumor progression from post-treatment effect (84).

Added Values of Multiparametric Imaging

The frequent co-existence of tumor recurrence and radiation injury in post-treatment brain tumor and the heterogeneous nature of the tumor, itself, represent substantial challenges to the evaluation of post-treatment lesions with single, quantitative parameters (85). A single parameter is only capable of providing a probability in one direction or a linear correlation, and which limits the comprehensive characterization of post-treatment tumors.

A proper combination of quantitative imaging parameters is likely to improve the discrimination power and tissue characterization in post-treatment brain tumors.

According to our previous study using all possible combinations of MR imaging modalities (77), adding DSC or DCE perfusion MR imaging to DWI significantly improved the diagnostic accuracy and interobserver agreement for distinguishing recurrent glioblastoma from radiation necrosis. This result suggests that the MR imaging protocol that includes conventional MR imaging, DWI, and any perfusion MR imaging is most efficient in the accurate determination of recurrent glioblastoma. For a voxel-by-voxel approach (Fig. 15), multiparametric imaging was a superior and more reproducible imaging biomarker than single parameter measurements for differentiating pseudoprogression from early tumor progression in patients with post-treatment glioblastoma. Therefore, a multifaceted segmentation approach can allow improved pathology characterization in brain tumor imaging (86).

CONCLUSIONS

Many currently available advanced imaging techniques may be optimally implemented to solve the diagnostic challenges of conventional MR imaging and to improve the tumor response assessment if their different pathophysiologic backgrounds and clinical impacts are understood. In addition, there is a variety of promising physiologic imaging techniques, such as APT and ASL, although they require further validation and standardization before being integrated into clinical practice for brain tumor imaging.

REFERENCES

1. Jahng GH, Li KL, Ostergaard L, Calamante F. Perfusion magnetic resonance imaging: a comprehensive update on principles and techniques. *Korean J Radiol* 2014;15:554-577
2. Park SH, Han PK, Choi SH. Physiological and functional magnetic resonance imaging using balanced steady-state free precession. *Korean J Radiol* 2015;16:550-559
3. Iima M, Le Bihan D. Clinical intravoxel incoherent motion and diffusion MR imaging: past, present, and future. *Radiology* 2016;278:13-32
4. Jensen JH, Helpern JA, Ramani A, Lu H, Kaczynski K. Diffusional kurtosis imaging: the quantification of non-gaussian water diffusion by means of magnetic resonance imaging. *Magn Reson Med* 2005;53:1432-1440
5. Hu LS, Eschbacher JM, Dueck AC, Heiserman JE, Liu S, Karis

JP, et al. Correlations between perfusion MR imaging cerebral blood volume, microvessel quantification, and clinical outcome using stereotactic analysis in recurrent high-grade glioma. *AJNR Am J Neuroradiol* 2012;33:69-76

6. Gilad AA, Israely T, Dafni H, Meir G, Cohen B, Neeman M. Functional and molecular mapping of uncoupling between vascular permeability and loss of vascular maturation in ovarian carcinoma xenografts: the role of stroma cells in tumor angiogenesis. *Int J Cancer* 2005;117:202-211

7. Ellingson BM, Malkin MG, Rand SD, Connelly JM, Quinsey C, LaViolette PS, et al. Validation of functional diffusion maps (fDMs) as a biomarker for human glioma cellularity. *J Magn Reson Imaging* 2010;31:538-548

8. Sugahara T, Korogi Y, Kochi M, Ikushima I, Shigematu Y, Hirai T, et al. Usefulness of diffusion-weighted MRI with echo-planar technique in the evaluation of cellularity in gliomas. *J Magn Reson Imaging* 1999;9:53-60

9. Filli L, Wurnig M, Nanz D, Luechinger R, Kenkel D, Boss A. Whole-body diffusion kurtosis imaging: initial experience on non-Gaussian diffusion in various organs. *Invest Radiol* 2014;49:773-778

10. LaViolette PS, Mickevicius NJ, Cochran EJ, Rand SD, Connelly J, Bovi JA, et al. Precise ex vivo histological validation of heightened cellularity and diffusion-restricted necrosis in regions of dark apparent diffusion coefficient in 7 cases of high-grade glioma. *Neuro Oncol* 2014;16:1599-1606

11. Choi H, Paeng JC, Cheon GJ, Park CK, Choi SH, Min HS, et al. Correlation of 11C-methionine PET and diffusion-weighted MRI: is there a complementary diagnostic role for gliomas? *Nucl Med Commun* 2014;35:720-726

12. Rose S, Fay M, Thomas P, Bourgeat P, Dowson N, Salvado O, et al. Correlation of MRI-derived apparent diffusion coefficients in newly diagnosed gliomas with [18F]-fluoro-L-dopa PET: what are we really measuring with minimum ADC? *AJNR Am J Neuroradiol* 2013;34:758-764

13. Hayashida Y, Hirai T, Morishita S, Kitajima M, Murakami R, Korogi Y, et al. Diffusion-weighted imaging of metastatic brain tumors: comparison with histologic type and tumor cellularity. *AJNR Am J Neuroradiol* 2006;27:1419-1425

14. Shim WH, Kim HS, Choi CG, Kim SJ. Comparison of apparent diffusion coefficient and intravoxel incoherent motion for differentiating among glioblastoma, metastasis, and lymphoma focusing on diffusion-related parameter. *PLoS One* 2015;10:e0134761

15. Federau C, Maeder P, O'Brien K, Browaeys P, Meuli R, Hagmann P. Quantitative measurement of brain perfusion with intravoxel incoherent motion MR imaging. *Radiology* 2012;265:874-881

16. Notohamiprodjo M, Chandarana H, Mikheev A, Rusinek H, Grinstead J, Feiweier T, et al. Combined intravoxel incoherent motion and diffusion tensor imaging of renal diffusion and flow anisotropy. *Magn Reson Med* 2015;73:1526-1532

17. Raab P, Hattingen E, Franz K, Zanella FE, Lanfermann H. Cerebral gliomas: diffusional kurtosis imaging analysis of microstructural differences. *Radiology* 2010;254:876-881

18. Dean BL, Drayer BP, Bird CR, Flom RA, Hodak JA, Coons SW, et al. Gliomas: classification with MR imaging. *Radiology* 1990;174:411-415

19. Falangola MF, Jensen JH, Babb JS, Hu C, Castellanos FX, Di Martino A, et al. Age-related non-Gaussian diffusion patterns in the prefrontal brain. *J Magn Reson Imaging* 2008;28:1345-1350

20. Kim SJ, Choi CG, Kim JK, Yun SC, Jahng GH, Jeong HK, et al. Effects of MR parameter changes on the quantification of diffusion anisotropy and apparent diffusion coefficient in diffusion tensor imaging: evaluation using a diffusional anisotropic phantom. *Korean J Radiol* 2015;16:297-303

21. Daumas-Duport C, Scheithauer B, O'Fallon J, Kelly P. Grading of astrocytomas. A simple and reproducible method. *Cancer* 1988;62:2152-2165

22. Maier SE, Sun Y, Mulkern RV. Diffusion imaging of brain tumors. *NMR Biomed* 2010;23:849-864

23. Iima M, Yano K, Kataoka M, Umehana M, Murata K, Kanao S, et al. Quantitative non-Gaussian diffusion and intravoxel incoherent motion magnetic resonance imaging: differentiation of malignant and benign breast lesions. *Invest Radiol* 2015;50:205-211

24. Birner P, Piribauer M, Fischer I, Gatterbauer B, Marosi C, Ambros PF, et al. Vascular patterns in glioblastoma influence clinical outcome and associate with variable expression of angiogenic proteins: evidence for distinct angiogenic subtypes. *Brain Pathol* 2003;13:133-143

25. Korkolopoulou P, Patsouris E, Kavantzas N, Konstantinidou AE, Christodoulou P, Thomas-Tsagli E, et al. Prognostic implications of microvessel morphometry in diffuse astrocytic neoplasms. *Neuropathol Appl Neurobiol* 2002;28:57-66

26. Wesseling P, van der Laak JA, Link M, Teepen HL, Ruiter DJ. Quantitative analysis of microvascular changes in diffuse astrocytic neoplasms with increasing grade of malignancy. *Hum Pathol* 1998;29:352-358

27. Wesseling P, van der Laak JA, de Leeuw H, Ruiter DJ, Burger PC. Quantitative immunohistological analysis of the microvasculature in untreated human glioblastoma multiforme. Computer-assisted image analysis of whole-tumor sections. *J Neurosurg* 1994;81:902-909

28. Barajas RF Jr, Phillips JJ, Parvataneni R, Molinaro A, Essock-Burns E, Bourne G, et al. Regional variation in histopathologic features of tumor specimens from treatment-naive glioblastoma correlates with anatomic and physiologic MR Imaging. *Neuro Oncol* 2012;14:942-954

29. Hyodo F, Chandramouli GV, Matsumoto S, Matsumoto K, Mitchell JB, Krishna MC, et al. Estimation of tumor microvessel density by MRI using a blood pool contrast agent. *Int J Oncol* 2009;35:797-804

30. Wilmes LJ, Pallavicini MG, Fleming LM, Gibbs J, Wang D, Li KL, et al. AG-013736, a novel inhibitor of VEGF receptor tyrosine kinases, inhibits breast cancer growth and decreases vascular permeability as detected by dynamic contrast-enhanced magnetic resonance imaging. *Magn Reson Imaging* 2007;25:319-327

31. Boxerman JL, Schmainda KM, Weisskoff RM. Relative cerebral blood volume maps corrected for contrast agent extravasation significantly correlate with glioma tumor grade, whereas uncorrected maps do not. *AJNR Am J Neuroradiol* 2006;27:859-867

32. Donahue KM, Krouwer HG, Rand SD, Pathak AP, Marszalkowski CS, Censky SC, et al. Utility of simultaneously acquired gradient-echo and spin-echo cerebral blood volume and morphology maps in brain tumor patients. *Magn Reson Med* 2000;43:845-853

33. Choi HS, Ahn SS, Shin NY, Kim J, Kim JH, Lee JE, et al. Permeability parameters measured with dynamic contrast-enhanced MRI: correlation with the extravasation of evans blue in a rat model of transient cerebral ischemia. *Korean J Radiol* 2015;16:791-797

34. Tofts PS. Modeling tracer kinetics in dynamic Gd-DTPA MR imaging. *J Magn Reson Imaging* 1997;7:91-101

35. Brix G, Griebel J, Kiessling F, Wenz F. Tracer kinetic modelling of tumour angiogenesis based on dynamic contrast-enhanced CT and MRI measurements. *Eur J Nucl Med Mol Imaging* 2010;37 Suppl 1:S30-S51

36. Patankar TF, Haroon HA, Mills SJ, Balériaux D, Buckley DL, Parker GJ, et al. Is volume transfer coefficient (K(trans)) related to histologic grade in human gliomas? *AJNR Am J Neuroradiol* 2005;26:2455-2465

37. Marzola P, Degrassi A, Calderan L, Farace P, Crescimanno C, Nicolato E, et al. In vivo assessment of antiangiogenic activity of SU6668 in an experimental colon carcinoma model. *Clin Cancer Res* 2004;10:739-750

38. Klemm F, Joyce JA. Microenvironmental regulation of therapeutic response in cancer. *Trends Cell Biol* 2015;25:198-213

39. Sorensen AG, Batchelor TT, Zhang WT, Chen PJ, Yeo P, Wang M, et al. A "vascular normalization index" as potential mechanistic biomarker to predict survival after a single dose of cediranib in recurrent glioblastoma patients. *Cancer Res* 2009;69:5296-5300

40. Jain RK. Normalizing tumor microenvironment to treat cancer: bench to bedside to biomarkers. *J Clin Oncol* 2013;31:2205-2218

41. Sorensen AG, Emblem KE, Polaskova P, Jennings D, Kim H, Ancukiewicz M, et al. Increased survival of glioblastoma patients who respond to antiangiogenic therapy with elevated blood perfusion. *Cancer Res* 2012;72:402-407

42. Detre JA, Zhang W, Roberts DA, Silva AC, Williams DS, Grandis DJ, et al. Tissue specific perfusion imaging using arterial spin labeling. *NMR Biomed* 1994;7:75-82

43. Noguchi T, Yoshiura T, Hiwatashi A, Togao O, Yamashita K, Nagao E, et al. Perfusion imaging of brain tumors using arterial spin-labeling: correlation with histopathologic vascular density. *AJNR Am J Neuroradiol* 2008;29:688-693

44. Warmuth C, Gunther M, Zimmer C. Quantification of blood flow in brain tumors: comparison of arterial spin labeling and dynamic susceptibility-weighted contrast-enhanced MR imaging. *Radiology* 2003;228:523-532

45. Haacke EM, Xu Y, Cheng YC, Reichenbach JR. Susceptibility weighted imaging (SWI). *Magn Reson Med* 2004;52:612-618

46. Mittal S, Wu Z, Neelavalli J, Haacke EM. Susceptibility-weighted imaging: technical aspects and clinical applications, part 2. *AJNR Am J Neuroradiol* 2009;30:232-252

47. Sehgal V, Delproposto Z, Haacke EM, Tong KA, Wycliffe N, Kido DK, et al. Clinical applications of neuroimaging with susceptibility-weighted imaging. *J Magn Reson Imaging* 2005;22:439-450

48. Barth M, Nöbauer-Huhmann IM, Reichenbach JR, Mlynárik V, Schöggl A, Matula C, et al. High-resolution three-dimensional contrast-enhanced blood oxygenation level-dependent magnetic resonance venography of brain tumors at 3 Tesla: first clinical experience and comparison with 1.5 Tesla. *Invest Radiol* 2003;38:409-414

49. Fahrendorf D, Schwindt W, Wölfer J, Jeibmann A, Kooijman H, Kugel H, et al. Benefits of contrast-enhanced SWI in patients with glioblastoma multiforme. *Eur Radiol* 2013;23:2868-2879

50. Sampetrean O, Saga I, Nakanishi M, Sugihara E, Fukaya R, Onishi N, et al. Invasion precedes tumor mass formation in a malignant brain tumor model of genetically modified neural stem cells. *Neoplasia* 2011;13:784-791

51. Jones CK, Schlosser MJ, van Zijl PC, Pomper MG, Golay X, Zhou J. Amide proton transfer imaging of human brain tumors at 3T. *Magn Reson Med* 2006;56:585-592

52. Henkelman RM, Stanisz GJ, Graham SJ. Magnetization transfer in MRI: a review. *NMR Biomed* 2001;14:57-64

53. van Zijl PC, Yadav NN. Chemical exchange saturation transfer (CEST): what is in a name and what isn't? *Magn Reson Med* 2011;65:927-948

54. Zhou J, Zhu H, Lim M, Blair L, Quinones-Hinojosa A, Messina SA, et al. Three-dimensional amide proton transfer MR imaging of gliomas: initial experience and comparison with gadolinium enhancement. *J Magn Reson Imaging* 2013;38:1119-1128

55. Togao O, Yoshiura T, Keupp J, Hiwatashi A, Yamashita K, Kikuchi K, et al. Amide proton transfer imaging of adult diffuse gliomas: correlation with histopathological grades. *Neuro Oncol* 2014;16:441-448

56. Sagiyama K, Mashimo T, Togao O, Vemireddy V, Hatanpaa KJ, Maher EA, et al. In vivo chemical exchange saturation transfer imaging allows early detection of a therapeutic response in glioblastoma. *Proc Natl Acad Sci U S A* 2014;111:4542-4547

57. Park JE, Kim HS, Park KJ, Kim SJ, Kim JH, Smith SA. Pre- and posttreatment glioma: comparison of amide proton transfer imaging with MR spectroscopy for biomarkers of tumor proliferation. *Radiology* 2016;278:514-523

58. Chenevert TL, McKeever PE, Ross BD. Monitoring early response of experimental brain tumors to therapy using diffusion magnetic resonance imaging. *Clin Cancer Res* 1997;3:1457-1466

59. Lee EK, Choi SH, Yun TJ, Kang KM, Kim TM, Lee SH, et al. Prediction of response to concurrent chemoradiotherapy with temozolomide in glioblastoma: application ofimmediate post-operative dynamic susceptibility contrast and diffusion-

weighted MR imaging. *Korean J Radiol* 2015;16:1341-1348

60. Ellingson BM, Sahebjam S, Kim HJ, Pope WB, Harris RJ, Woodworth DC, et al. Pretreatment ADC histogram analysis is a predictive imaging biomarker for bevacizumab treatment but not chemotherapy in recurrent glioblastoma. *AJNR Am J Neuroradiol* 2014;35:673-679

61. High WA, Ayers RA, Cowper SE. Gadolinium is quantifiable within the tissue of patients with nephrogenic systemic fibrosis. *J Am Acad Dermatol* 2007;56:710-712

62. Kanda T, Ishii K, Kawaguchi H, Kitajima K, Takenaka D. High signal intensity in the dentate nucleus and globus pallidus on unenhanced T1-weighted MR images: relationship with increasing cumulative dose of a gadolinium-based contrast material. *Radiology* 2014;270:834-841

63. Kim DY, Kim HS, Goh MJ, Choi CG, Kim SJ. Utility of intravoxel incoherent motion MR imaging for distinguishing recurrent metastatic tumor from treatment effect following gamma knife radiosurgery: initial experience. *AJNR Am J Neuroradiol* 2014;35:2082-2090

64. Kim HS, Suh CH, Kim N, Choi CG, Kim SJ. Histogram analysis of intravoxel incoherent motion for differentiating recurrent tumor from treatment effect in patients with glioblastoma: initial clinical experience. *AJNR Am J Neuroradiol* 2014;35:490-497

65. Bai Y, Lin Y, Tian J, Shi D, Cheng J, Haacke EM, et al. Grading of gliomas by using monoexponential, biexponential, and stretched exponential diffusion-weighted MR imaging and diffusion kurtosis MR imaging. *Radiology* 2016;278:496-504

66. Van Cauter S, Veraart J, Sijbers J, Peeters RR, Himmelreich U, De Keyzer F, et al. Gliomas: diffusion kurtosis MR imaging in grading. *Radiology* 2012;263:492-501

67. Brandsma D, Stalpers L, Taal W, Sminia P, van den Bent MJ. Clinical features, mechanisms, and management of pseudoprogression in malignant gliomas. *Lancet Oncol* 2008;9:453-461

68. Sanghera P, Perry J, Sahgal A, Symons S, Aviv R, Morrison M, et al. Pseudoprogression following chemoradiotherapy for glioblastoma multiforme. *Can J Neurol Sci* 2010;37:36-42

69. Kong DS, Kim ST, Kim EH, Lim DH, Kim WS, Suh YL, et al. Diagnostic dilemma of pseudoprogression in the treatment of newly diagnosed glioblastomas: the role of assessing relative cerebral blood flow volume and oxygen-6-methylguanine-DNA methyltransferase promoter methylation status. *AJNR Am J Neuroradiol* 2011;32:382-387

70. Chamberlain MC. Pseudoprogression in glioblastoma. *J Clin Oncol* 2008;26:4359; author reply 4359-4360

71. Baek HJ, Kim HS, Kim N, Choi YJ, Kim YJ. Percent change of perfusion skewness and kurtosis: a potential imaging biomarker for early treatment response in patients with newly diagnosed glioblastomas. *Radiology* 2012;264:834-843

72. Wang S, Martinez-Lage M, Sakai Y, Chawla S, Kim SG, Alonso-Basanta M, et al. Differentiating tumor progression from pseudoprogression in patients with glioblastomas using diffusion tensor imaging and dynamic susceptibility contrast MRI. *AJNR Am J Neuroradiol* 2016;37:28-36

73. Mangla R, Singh G, Ziegelitz D, Milano MT, Korones DN, Zhong J, et al. Changes in relative cerebral blood volume 1 month after radiation-temozolomide therapy can help predict overall survival in patients with glioblastoma. *Radiology* 2010;256:575-584

74. Radbruch A, Bendszus M, Wick W, Heiland S. Comment to: parametric response map as an imaging biomarker to distinguish progression from pseudoprogression in high-grade glioma: pitfalls in perfusion MRI in brain tumors: Tsien C, Galbán CJ, Chenevert TL, Johnson TD, Hamstra DA, Sundgren PC, Junck L, Meyer CR, Rehemtulla A, Lawrence T, Ross BD. J Clin Oncol. 2010;28:2293-9. *Clin Neuroradiol* 2010;20:183-184

75. Cheng HL, Wallis C, Shou Z, Farhat WA. Quantifying angiogenesis in VEGF-enhanced tissue-engineered bladder constructs by dynamic contrast-enhanced MRI using contrast agents of different molecular weights. *J Magn Reson Imaging* 2007;25:137-145

76. Leach MO, Brindle KM, Evelhoch JL, Griffiths JR, Horsman MR, Jackson A, et al. Assessment of antiangiogenic and antivascular therapeutics using MRI: recommendations for appropriate methodology for clinical trials. *Br J Radiol* 2003;76 Spec No 1:S87-S91

77. Kim HS, Goh MJ, Kim N, Choi CG, Kim SJ, Kim JH. Which combination of MR imaging modalities is best for predicting recurrent glioblastoma? Study of diagnostic accuracy and reproducibility. *Radiology* 2014;273:831-843

78. Narang J, Jain R, Arbab AS, Mikkelsen T, Scarpace L, Rosenblum ML, et al. Differentiating treatment-induced necrosis from recurrent/progressive brain tumor using nonmodel-based semiquantitative indices derived from dynamic contrast-enhanced T1-weighted MR perfusion. *Neuro Oncol* 2011;13:1037-1046

79. Li C, Ai B, Li Y, Qi H, Wu L. Susceptibility-weighted imaging in grading brain astrocytomas. *Eur J Radiol* 2010;75:e81-e85

80. Park MJ, Kim HS, Jahng GH, Ryu CW, Park SM, Kim SY. Semiquantitative assessment of intratumoral susceptibility signals using non-contrast-enhanced high-field high-resolution susceptibility-weighted imaging in patients with gliomas: comparison with MR perfusion imaging. *AJNR Am J Neuroradiol* 2009;30:1402-1408

81. Pinker K, Noebauer-Huhmann IM, Stavrou I, Hoeftberger R, Szomolanyi P, Karanikas G, et al. High-resolution contrast-enhanced, susceptibility-weighted MR imaging at 3T in patients with brain tumors: correlation with positron-emission tomography and histopathologic findings. *AJNR Am J Neuroradiol* 2007;28:1280-1286

82. Hori M, Ishigame K, Kabasawa H, Kumagai H, Ikenaga S, Shiraga N, et al. Precontrast and postcontrast susceptibility-weighted imaging in the assessment of intracranial brain neoplasms at 1.5 T. *Jpn J Radiol* 2010;28:299-304

83. Park JE, Kim HS, Park KJ, Choi CG, Kim SJ. Histogram analysis of amide proton transfer imaging to identify contrast-enhancing low-grade brain tumor that mimics high-grade tumor: increased accuracy of MR perfusion. *Radiology* 2015;277:151-161

84. Park KJ, Kim HS, Park JE, Shim WH, Kim SJ, Smith SA. Added value of amide proton transfer imaging to conventional and perfusion MR imaging for evaluating the treatment response of newly diagnosed glioblastoma. *Eur Radiol* 2016 Feb 16 [Epub]. http://dx.doi.org/10.1007/s00330-016-4261-2

85. Jung V, Romeike BF, Henn W, Feiden W, Moringlane JR, Zang KD, et al. Evidence of focal genetic microheterogeneity in glioblastoma multiforme by area-specific CGH on microdissected tumor cells. *J Neuropathol Exp Neurol* 1999;58:993-999

86. Park JE, Kim HS, Goh MJ, Kim SJ, Kim JH. Pseudoprogression in patients with glioblastoma: assessment by using volume-weighted voxel-based multiparametric clustering of MR imaging data in an independent test set. *Radiology* 2015;275:792-802